This is a non-peer-reviewed preprint submitted to EarthArxiv, currently in review at Geophysical Journal International

Assessment of a claimed ultra-low frequency electromagnetic (ULFEM) earthquake precursor

Can Wang[1,2,3], Lilianna E. Christman[1,2], Simon L. Klemperer[2], Jonathan M. Glen[1], Darcy K. McPhee[4], Bin Chen[1,3]

[1]U.S. Geological Survey, Menlo Park, CA 94025, USA
[2]Department of Geophysics, Stanford University, CA 94305-2215, USA
[3]Institute of Geophysics, China Earthquake Administration, Beijing 100081, P.R. China
[4]U.S. Geological Survey, Reston, VA 20192, USA

Dates: April 2021
Short title: Test of ULFEM earthquake precursors

Contact authors: Can Wang, wangcan0312@cea-igp.ac.cn,
Simon Klemperer, sklemp@stanford.edu

SUMMARY

Anomalous ultra-low frequency electromagnetic (ULFEM) pulses occurring before the M5.4 2007 and M4.0 2010 Alum Rock earthquakes have been claimed to increase in number days to weeks prior to each earthquake. We re-examine the previously reported ultra-low frequency (ULF: 0.01-10 Hz) magnetic data recorded at a QuakeFinder site located 9 km from the earthquake hypocenter, as well as data from a nearby Stanford-USGS site located 42 km from the hypocenter, to analyze the characteristics of the pulses and assess their origin. Using pulse definitions and pulse-counting algorithms analogous to those previously reported, we corroborate the increase in pulse counts before the 2007 Alum Rock earthquake at the QuakeFinder station, but we note that the number of pulses depends greatly on chosen temporal and amplitude detection thresholds. These thresholds are necessarily arbitrary because we lack a clear physical model or basis for their selection. We do not see the same increase in pulse counts before the 2010 Alum Rock earthquake at the QuakeFinder or Stanford-USGS station. In addition, when comparing specific pulses in the QuakeFinder data and Stanford-USGS data, we find that the majority of pulses do not match temporally, indicating the pulses are not from solar-driven ionospheric/magnetospheric disturbances or from atmospheric lightning, and lack a common origin. Notably, however, our assessment of the temporal distribution of pulse counts throughout the day shows pulse counts increase during peak human activity hours, strongly suggesting these pulses result from local cultural noise and are not tectonic in origin. The many unknowns about the character and even existence of precursory earthquake pulses means that otherwise standard numerical and statistical test cannot be applied. Yet here we show that exhaustive investigation of many different aspects of ULFEM signals can be used to properly characterize their origin.

Keywords: earthquake precursor, ultra-low frequency, time-series analysis, probabilistic forecasting, magnetic field, Earthquake early warning

1 INTRODUCTION

Numerous papers have reported anomalous signals occurring in ultra-low frequency electromagnetic (ULFEM: 0.01-10 Hz) data prior to earthquakes. The most highly cited observations were made prior to the 1989 M7.1 Loma Prieta earthquake (Fraser-Smith et al., 1990), ranging from a narrow-band signal (0.05 – 0.2 Hz) starting about a month before the earthquake to a dramatic enhancement of broadband activity (0.01 – 0.5 Hz) approximately three hours before the earthquake. Fraser-Smith et al. (1990) concluded that these anomalous signals were most likely magnetic precursors to the Loma Prieta earthquake, an assertion that has been controversial (Campbell, 2009 vs. Fraser-Smith et al., 2011; Thomas et al., 2007 vs. Culp et al., 2007; Thomas et al., 2009a; Thomas et al. 2013 vs. Fraser-Smith et al., 2013). The claimed ULFEM precursors to the Loma Prieta earthquake largely inspired recent global efforts to monitor telluric ULFEM fields, including our own Stanford-USGS array in California (Wang et al., 2018). Other notable results include reports – and rebuttals – of anomalous signals months to hours before the M6.9 Spitak 1998 earthquake (Kopytenko et al., 1993), the M7.1 Guam 1993 earthquake (Hayakawa et al., 1996; Thomas et al., 2009b), the M8.0 Wenchuan 2008 earthquake (Li et al., 2013), the M7.6 Chi Chi Taiwan 1999 earthquake (Liu et al., 2006; Tsai et al., 2006; Masci, 2011), and the M9.0 Tohoku 2011 earthquake (Xu et al., 2013). Furthermore, there are a number of clear failures of this technique to detect precursors to well-instrumented earthquakes such as the M6.0 Parkfield 2004 earthquake (Johnston et al., 2006), the M7.1 Hector Mine 1999 earthquake (Karakelian et al., 2002) and the M8.8 Chilean 2010 earthquake (Romanova, et al., 2015). A review of earthquake precursors (Cicerone et al., 2009) shows fewer claimed precursors associated with smaller earthquakes, $M \leq 5$, but suggestions of precursory ULFEM signals have been made related to aftershock sequences (e.g., Fenoglio et al., 1993), isolated small earthquakes (Masci et al., 2009) and swarm activity (e.g., Kolar, 2010), as well as to the Alum Rock earthquakes (Bleier et al., 2009; Dunson et al., 2011) further discussed here. A continuing issue in the field is the problem of recognizing ionospheric and magnetospheric disturbance signals and removing these from the data (e.g., Masci, 2011; Wang et al., 2018) or distinguishing them from potential tectonic signals. Reduction of both ionospheric and magnetospheric disturbance noise in magnetic array data has been a research field for the last 50 years. The basic techniques were developed in the USGS 80-station magnetometer network installed along the San Andreas Fault system from 1972 to 2002 (Mueller & Johnston, 1997; Johnston, 1998; Johnston et al., 1984; Ware et al., 1985; Davis et al., 1980, 1983). With these techniques, external disturbance fields can be reduced by a factor of about 100. Using the 80-station USGS array, just one apparent magnetic precursor (~3nT) was observed (on three independent stations) in 30 years of monitoring (Davis et al., 1980) but co-seismic changes (0.1-3 nT) were routinely observed for earthquakes with M>6 that are consistent with the earthquake source mechanism, stress drop and distance (e.g. Johnston et al., 2006, M6 Parkfield earthquake in 2004). Without noise reduction, the very existence of ULFEM precursors to earthquakes remains open to question.

We categorize the signals that appear in ULFEM data into four general types, 1) atmospheric signals, which we use to mean from all atmospheric, ionospheric, and magnetospheric sources; 2) tectonic signals, representing any natural signal that comes from inside the earth, including those generated from tectonic or water movement; 3) cultural signals, referring to all anthropogenic or animal-related signals, such as cars, water pumps, animals, etc.; and 4) instrumental signals, or those generated internally by the system, such as responses to power spikes.

In this paper we focus on the observation that anomalous tectonically-sourced magnetic pulsations occurred prior to the Oct 31, 2007 Alum Rock M5.4 earthquake near San Jose, California (hereafter “AR2007”; Table 1, Fig. 1), with an increase in pulse counts peaking two weeks before the earthquake and then a dip in pulse counts about one day before the event (Bleier et al., 2009). Bleier et al. (2009) counted pulses that exceeded a threshold determined by a site-specific background noise and saw increased numbers of pulses on a single QuakeFinder site (East Milpitas / QF609), 2 km distant from the epicenter (Table 2, Fig. 1). Although QuakeFinder

Inc. maintains a relatively large and dense array of ULFEM stations (CalMagNet, Cutler et al., 2008), the next closest QuakeFinder site to the Alum Rock earthquake, in Portola Valley 38 km west of the epicenter (Fig. 1), did not detect any increase in pulses (Bleier et al., 2009). This is an example of one of the challenges of this field described above: ensuring stations in arrays are close enough for at least two stations to record possible signals related to earthquake events. An analogous increase in pulse activity prior to the Jan 07, 2010 Alum Rock M4.0 earthquake (hereafter "AR2010"; Table 1, Fig. 1) has been reported at the same QF609 site (Dunson et al., 2011).

Table 1: Parameters of earthquakes studied

	AR2007	AR2010
Date	October 31, 2007	January 7, 2010
Location	37.432°N, 121.776°W	37.4765°N, 121.797°W
Depth	9.2 km	9 km
Magnitude	5.4	4.0

All values adopted from Bleier et al. (2009) and Dunson et al. (2011)

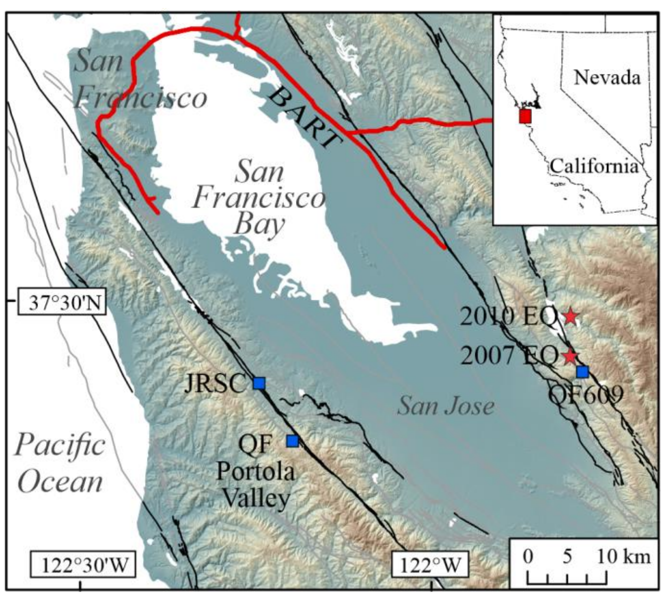

Figure 1: Shaded-relief topographic map of the San Francisco Bay Area, California. JRSC, QF609 and QF Portola Valley ULFEM sites are shown by blue squares. The 2007 and 2010 Alum Rock earthquakes (red stars) occurred along the Calaveras Fault. Black and grey lines: major and minor faults. Red lines: BART electric train.

Stanford, USGS and UC Berkeley have collaborated to maintain five ULFEM recording sites along strands of the San Andreas Fault system in the San Francisco Bay Area (e.g., Bijoor et al., 2005; Neumann et al., 2008; Wang et al., 2018). The closest Stanford-USGS site to the Alum Rock earthquake is JRSC, at the Jasper Ridge Biological Preserve, 41 km from the AR2007 epicenter (Table 2, Fig. 1). We examined data from this site, JRSC, and re-examined the data from QF609 presented by Bleier et al. (2009) for AR2007 and Dunson et al. (2011) for AR2010. Although JRSC and QF609 utilize different magnetometers and digitizers, a comparison of the two systems shows they have similar signal responses.

Table 2: Parameters of ULF stations utilized

	JRSC	**QF609**	**FRN**
Latitude °N, longitude °E	37.403, -122.239	37.416, -121.780	37.091, -119.719
Effective bandwidth	1000s-15 Hz	1000s-12 Hz	1000s-0.5 Hz
Magnetometer type	BF-4 magnetic field induction coil, Schlumberger	Ant/4 magnetic field induction coil, Zonge International	Narod fluxgate magnetometer
Sample rate	40 Hz	32 Hz	1 Hz
Digitizer	24-bit Quanterra data-logger	24-bit A/D Symmetric Research Inc.	N/A
Additional data channels, not studied in this paper	• Total-field magnetometer sampled at 10 Hz (Geometrics) • Orthogonal 100-m electrodes • Broadband seismometer (Northern California Seismic Network)	• 4 Hz geophone • Air conductivity sensor -Temperature and humidity	N/A
Distance to AR2007 hypocenter (epicenter)	42 km (41 km)	9 km (2 km)	185 km (185 km)
Distance to AR2010 hypocenter (epicenter)	41 km (40 km)	11 km (7 km)	188 km (188 km)

In this paper, we present a pulse analysis of ultra-low frequency (ULF) magnetic data before and after the 2007 and 2010 Alum Rock earthquakes. We aim to assess the data and pulse counting methods of Bleier et al. (2009), attempt to reproduce their results and those of Dunson et al. (2011), and analyze pulse statistics. A listing of the times of the $>10^4$ pulses counted by

Bleier et al. (2009) is no longer available for study, but instead the raw data were generously provided by QuakeFinder Inc. for our re-evaluation. We apply a similar analysis matching the criteria used by Bleier et al. (2009), and then compare our pulse count results with those of Bleier et al. (2009). We show that the number of pulses and the time-variation of the rate of pulse occurrence are very sensitive to the precise parameters of the pulse-counting algorithm. With an appropriate choice of parameters we can confirm the existence of the increased pulse counts at QF609 shown by Bleier et al. (2009), but find no changes in pulse counts at JRSC for either the 2007 and the 2010 earthquakes. The difference in these two records suggests that either the pulses are attenuated below background noise levels before reaching the Stanford-USGS site, or they are not earthquake related. The latter seems likely since 1) no signals were observed at the time of the earthquake when the major energy and stress release occurs and 2) nothing in earthquake physics or observations indicates large signals should occur before earthquakes if no signals occur during earthquakes.

2 MEASUREMENT SYSTEMS AND RESOLUTION

The Stanford-USGS ultra-low frequency electromagnetic sites have three orthogonal induction coil magnetometers, aligned geomagnetically east-west, north-south and vertically, as well as two orthogonal horizontal electrode pairs in the east-west and north-south directions (Table 2). The Stanford-USGS stations are collocated with broadband seismometers to separate telluric signals from signals induced by seismic shaking (Karakelian et al., 2000; 2002). QuakeFinder stations consist of three orthogonal magnetometers, aligned geomagnetically east-west, north-south and vertically, but no electrodes. QuakeFinder stations, including QF609, also record the output of 4 Hz geophones (to monitor high-frequency ground motion), ion density, and basic weather information (Table 2) (Cutler et al., 2008; Bleier et al., 2009). A major source of ULF electromagnetic noise in the San Francisco Bay Area is the Bay Area Rapid Transit system, BART, a direct-current system with a ground return (e.g., Fraser-Smith & Coates, 1978; Liu &

Fraser-Smith, 1996), shown in Fig. 1. At JRSC, background signal levels during the hours of BART operation are an order-of-magnitude greater than when the system is not in operation, typically 02:00-04:00 clock time (CT, clock time in the San Francisco Bay Area is ~20 minutes ahead of local (solar) time in winter, and ~80 minutes early during summer 'Daylight Savings Time') (Karakelian et al., 2000; Bijoor et al., 2005). We therefore also use USGS magnetic observatory station FRN (Fresno, Table 2) as a remote reference station to corroborate results from within the San Francisco Bay Area (QF609 and JRSC), and whenever possible show data examples recorded during the 'quiet time' (BART off).

3 QUAKEFINDER CLAIMED EARTHQUAKE PRECURSOR

Bleier et al. (2009) reported an increase in long duration (1-30 seconds), high-amplitude (3–20 nT) pulses in their ULF magnetic data starting one to two months before the AR2007 earthquake. Pulse counts (number of qualifying pulses per unit time) peaked 13 days before the earthquake and then decreased slightly in the remaining days before the earthquake. The amplitudes of these pulses were 10–1000 times larger than the average ambient site noise.

Bleier et al. (2009) found these increases in the rate of occurrence of pulses using their own customized pulse-counting algorithm. They set an amplitude "threshold level" of "twice the largest noise signatures typically observed each day at each site", a value that in practice counted typically 0–15 pulses a day. Bleier et al. (2009) counted pulses that exceeded this threshold level, and monitored their duration polarity (positive unipolar, negative unipolar, or bi-polar with both positive and negative excursions exceeding the threshold). Bleier et al. (2009) discarded time periods contaminated by calibration signals (twice per day) and known man-made interference (including 6.5 hours during the period of increased pulse rate in October prior to the earthquake). Bleier et al. (2009) were also able to discount several possible causes for the increase in rates of pulse occurrence before the earthquake: solar-generated ULF sources were excluded because pulse counts were not consistent across multiple widely spaced network stations. We note, however, that disturbances will not be exactly the same at different sites because of induced signals that are locally generated by local magnetic structure and electrical conductivity, though they will occur at the same time across the network.Local lightning sources were excluded based on comparison with commercial lightning catalogs, and additionally mitigated against by only counting pulses longer than 1 second; and internal instrument noise was excluded by detecting identical pulses on a nearby station deployed temporarily after the AR2007 earthquake. A total of 11623 pulses were counted by Bleier et al. (2009) at QF609 from 5–31 October 2007 (430 per day), a rate 10 times the average rate over the entire 2006–2007 two-year period, and a rate 15 times the average rate excluding the pre-earthquake period of 5–31 October.

Dunson et al. (2011) extended the Bleier et al. (2009) analysis to include “direction-finding” (amplitude ratios of different orthogonal components of the magnetic field variations), and also reported increased pulse counts (with a slightly modified counting algorithm) both prior to the AR2007 magnitude 5.4 earthquake and also prior to the AR2010 magnitude 4.0 earthquake. In this analysis we attempt to reproduce the Bleier et al. (2009) results using a pulse-counting algorithm based on their reported methodology, and we apply the same methodology to our own JRSC dataset, and to both the 2007 and 2010 earthquakes. For simplicity we focus only on the west-east-oriented magnetometer channel that has the most continuous data record.

4 DATA ANALYSIS at QF609 and JRSC

4.1 Network Comparison Test

Before attempting to compare the historical (2007-2010) data from QuakeFinder and USGS-Stanford systems that use different coils, digitizers and telemetry (Table 2), we first collocated a temporary QuakeFinder installation at the JRSC station for two months. Analysis of the resultant data and contemporaneous records from remote reference FRN shows good coherence between the systems over long time periods, for ionospheric magnetic signals (continuous Pc and irregular Pi geomagnetic pulsations) that are expected to be regionally uniform, and most important for specific pulses similar to those counted in this study (Wang et al., 2018). However, occasional pulses that only occur on a single component sensor or single system (either QuakeFinder or JRSC) indicate that some anomalies are artifacts of system noise (e.g., power, digitizer, amplifier in the case of system-wide signals), or local ground disturbances (e.g., we suspect rodent burrowing in the case of single-sensor signals) (Wang et al., 2018).

4.2 Pulse Comparison between stations

In addition to the well-understood ionospheric signals, both JRSC and QF609 record examples of all the types of pulses that Bleier et al. (2009) described as unexplained by “contamination sources”: amplitude excursions of 1 to 30 seconds duration, unipolar positive, negative and bipolar, that clearly exceed the average noise levels (Fig. 2). If two recording sites are close enough to one another *and* to the source of the pulses, the pulses should appear on both systems. However, because we lack a physical mechanism for the observed pulses, we are uncertain how their amplitudes might scale with distance from their source. We expect the amplitude of the magnetic field to decrease with distance from its source (r) due to geometric spreading, and due to propagation through the Earth. This latter effect is often characterized by the skin depth z_s of the medium, or distance over which a signal is attenuated by a factor *e*. z_s^2 is proportional to the resistivity of the medium and to the period of the electromagnetic signal.

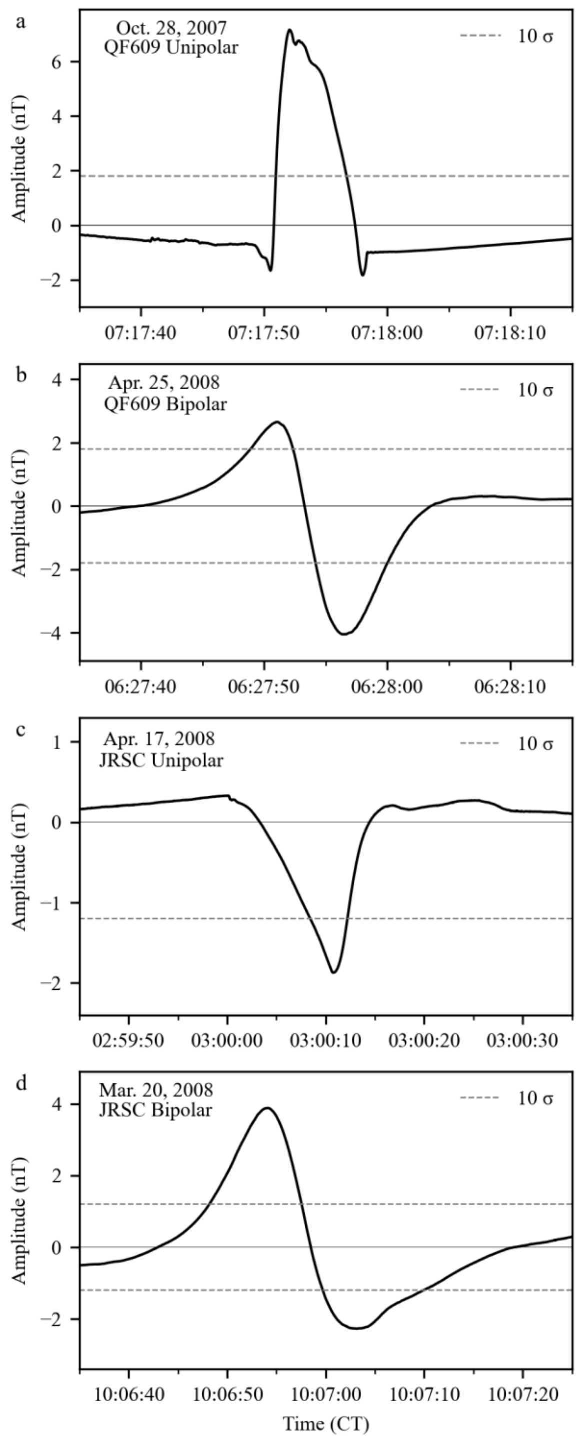

Figure 2: Examples of typical pulses at QF609 and JRSC, all on the east-west magnetometer. (a) Unipolar positive pulse on QF609, October 28, 2007. (b) Bipolar pulse on QF609, April 25, 2008. (c) Unipolar negative pulse on JRSC, April 17, 2008. (d) Bipolar pulse on JRSC, March 20, 2008. In all cases, the peaks of the pulses exceed a 10σ threshold (dashed lines), calculated separately for each station. All times are given in clock time (CT) after correction, if needed, for daylight savings time.

We assume the simplest likely source of the pulsations is a dipole, for which the amplitude decreases as r^3. More complex sources have more rapid decay rates, e.g., the amplitude of a quadrupole decreases as r^4. Attenuation is negligible in the atmosphere, but the Earth's skin depth is of the order of 1–10 km for 1 s periods assuming resistivities of ~4-400 ohm-m, realistic shallow crustal resistivities for this area (Eberhart-Phillips et al., 1990; Bedrosian et al., 2002). Our simplest model ignores any preferential directivity of the source and any signal loss at the earth-atmosphere interface.

If we assume a dipole source at the Alum Rock hypocenter (Fig. 3) and ignore attenuation (i.e., assume infinite skin depth) the ratio of signals at QF609 and at JRSC would be $(9\text{km}/42\text{km})^{-3} \approx 10^2$. With a skin depth of ~10 km (appropriate for conductivities of 10–100 mS/m and frequencies of 0.1–1 Hz), the ratio of signals at QF609 and at JRSC would be $(9\text{km}/42\text{km})^{-3}(e^{-1}/e^{-4}) \approx 10^3$ assuming lossy transmission along direct pathways through the earth; or $\{(9+2)/(9+41)\}^{-3} \approx 10^2$ assuming lossy vertical transmission in the earth and loss-free radial transmission in the atmosphere (Fig. 3). These ratios would decrease if the dipole source were placed further from QF609 and closer to JRSC than the Alum Rock hypocenter ("hypothetical alternate source" in Fig. 3). FRN is ~180 km from QF609, and ~225 km from JRSC, and pulses originating close to the Alum Rock hypocenter should be reduced by a factor of ~10^4–10^8 from their amplitude at QF609.

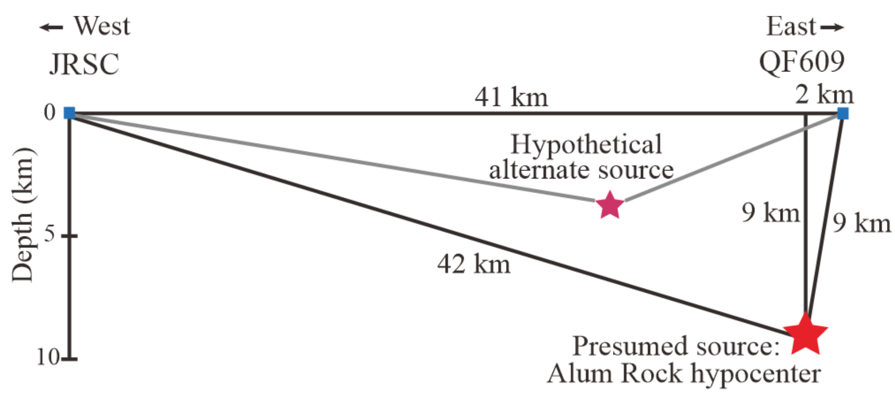

Figure 3: Simplified geometry of the relationship of JRSC, QF609 and the hypocenter and epicenter of the 2007 Alum Rock earthquake.

We tested whether any of the largest pulses reported in QF609 data were visible in JRSC data (or FRN data). For example, a large pulse recorded at QF609 (Fig. 4a) has no equivalent corresponding pulse at JRSC or at FRN at the same time as the QF609 pulse (Fig. 4c) so cannot have an ionospheric or magnetospheric source (Wang et al., 2018). Additionally, because the pulse is not present at JRSC even at an amplitude reduced from the QF609 amplitude by 10^3 (our estimated maximum attenuation) (Fig. 4c), this pulse is probably not generated at the Alum Rock hypocenter. Hence this pulse is likely either an artifact of instrument noise, or a local cultural source, or generated within the earth much closer to QF609 than the eventual AR2007 hypocenter.

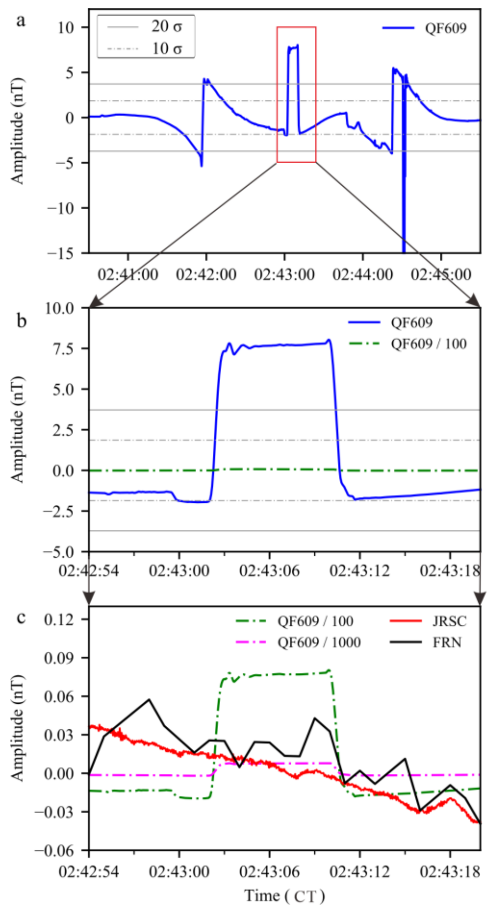

Figure 4: (a) Three pulses in QF609 east-west magnetometer data from October 30, 2007 (modified from Fig. 2d of Bleier et al., 2009). Dot-dashed and solid gray lines represent the threshold (10σ and 20σ) used to count pulses at QF609. (b) The middle pulse shown in more detail, and also reduced by a factor of 100 (dot-dashed green line) to represent possible scaling relationships at JRSC. (c) JRSC data (red solid line) and Fresno data (black solid line) for the same time period overlain by QF609 data scaled by 100 (green dot-dash lines) and by 1000 (pink dot-dash lines).

4.3 Pulse Counting

Even if individual pulses cannot be reliably identified on both JRSC and QF609, it is possible that a statistical test – comparing pulse counts over different time intervals – might show evidence of a coherent signal at JRSC. In this section we first show how we approximate the pulse-counting algorithm of Bleier et al. (2009) and then apply our algorithm to the two Alum Rock earthquakes.

4.3.1 Design of and parameter selection for pulse-counting algorithm

We counted pulses in QF609 and JRSC data both before and after the Oct 31 AR2007 earthquake, from Jan 1, 2007 through April 30, 2008. We analyzed all available channels but all plots in this paper are from the east-west magnetometer of each site, as reported by Bleier et al. (2009). We first designed a pulse-counting algorithm as similar as possible to the published description of Bleier et al. (2009) to test whether there was any increase in pulses at JRSC prior to the Alum Rock earthquake, and then we explored how changing the algorithm can give different results.

Bleier et al. (2009) noted the presence of some cultural noise (e.g., tractors working around site QF609), and manually removed these artifacts, as well as their calibration signals at noon and midnight. The list of times of known noise corrupting the QF609 data-set is given in Table 2 of Dunson et al. (2011), and we followed Bleier et al. (2009) in excluding these times from our pulse counting (Fig. 5a). There were nearly 100 days when one or the other site was malfunctioning or not recording data, reflecting the challenges of maintaining such a network in an urban setting; those full days were not examined in either data set in order to keep the datasets comparable (Table S1; Fig. 5b, Fig. S1).

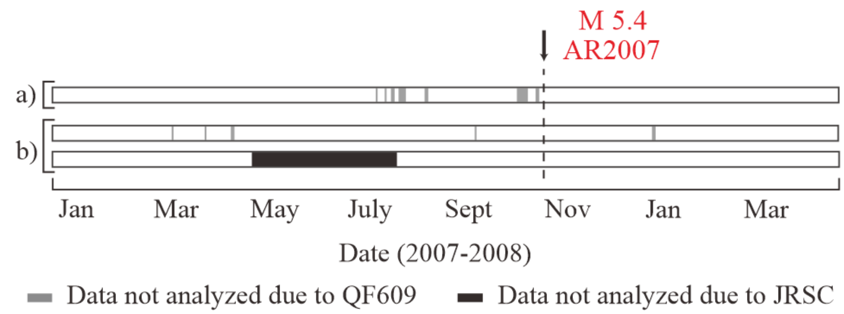

Figure 5: Timeline of data showing data analyzed in this study. Gray (bad QF609 data) and black (bad JRSC data) segments show data not analyzed. (a) Dunson et al. (2011) reported periods of data that were removed due to known site contamination (their Table 2), ranging from 1 minute to 8 hours, shown in gray. (b) Whole days removed by us due to large segments (>12 hours) of missing data from that day.

It is noteworthy that the incidence of even short periods of contaminated data due to cultural noise increases in the months before the earthquake. This increase in the number of contaminated periods may be real, or may represent the ability of Bleier et al. (2009) and Dunson et al. (2011) to retrospectively identify cultural events after the earthquake; it is easier to confirm specific hours of cultural activity, such as farm work or construction, that occurred a week ago compared to a year ago.

Our pulse definition parallels that described in Bleier et al. (2009). We bandpassed the QF609 and JRSC data using a Butterworth filter from 0.01 Hz to the cutoff of the anti-alias filter for QF609, 12 Hz, then removed the instrument responses (Fig. S2) to convert units of instrument counts in which the data are archived to units of nanotesla, nT. Next, we estimated the background noise at each station, to enable us to set an amplitude threshold above which we identify pulses. Our pulse-counting algorithm considered and distinguished unipolar positive, unipolar negative, and bipolar spikes. We examined 24 hours of data each day (00:01 to 23:59 clock time), and the total number of pulses counted each day is our reported pulse count. In the 387 days we pulse-counted for AR2007, the longest segment of data removed from QF609 was 45 minutes (Fig. 5a; Dunson et al., 2011), or only 3% of one day, so we did not bother to correct our reported pulse counts per day for this effect.

Our pulse counts are then defined by (1) the background noise based on an estimate of the standard deviation σ (calculated assuming the data are normally distributed); (2) the multiple of the standard deviation (M) we use as our amplitude threshold; and (3) the minimum duration T for which the amplitude must exceed the threshold $M\sigma$ to be counted as a pulse (to discriminate against much shorter-duration features such as local lightning in the data). Bleier et al. (2009) used an on-site test at QF609 to measure the effects of near-by equipment (pumps, welders, etc.) on signal levels, and set their threshold at twice the largest signal they observed due to these cultural sources of noise. We approximate this approach by a judicious choice of M. All pulses counted by Bleier et al. (2009) exceed the threshold for at least one sample (1/32 of a second, T ~ 0.03 s), and up to about 30 s. Bleier et al. (2009) discussed whether lightning might cause some short-period (< 1 s) pulses, and so although Beier et al. (2009) used no minimum duration T, we explore the effect on pulse counts of minimum T as high as 4 s. Note that for computational simplicity we follow Dunson et al. (2011, their Fig. 5) (and hence, we assume, also the method of Bleier et al. (2009)) in measuring pulse duration as the length of time for which the pulse amplitude exceeds the amplitude threshold. The dominant period of the pulse might be two to four times its measured duration, depending on the pulse shape and whether its amplitude barely or significantly exceeds the threshold.

In this study we define a pulse as that which exceeds $M\sigma$. We estimated σ in two ways: first as the deviation of the entire data set under consideration; and second by calculating the deviation of each day (or each 2-hour quiet period, while BART is non-operational) individually and then averaging the individual deviations over all days (or quiet times) being considered. The second approach gives a lower estimate of σ, as it averages over quiet time periods with little anthropogenic noise. For constant values of M and minimum duration T = 0.03 s, the number of pulses counted using either approach is different (Fig. S3) but the two methods show almost identical patterns across days. For the remainder of our analysis we chose the second method, averaging σ values obtained on different days or quiet periods, because it was computationally simpler when changing the analysis period over which we counted pulses (Table S2, Fig. S3).

For QF609 we tested different values of M (Fig. 6a); as expected, lower values of M increase the number of pulses detected. We tested different values of T (Figs. 6b and c); as expected lower values of T increase the number of pulses detected. Equivalent tests for JRSC are shown in Fig. S4. Table 3 reports the average apparent pulse rates at QF609 and JRSC for each combination of temporal threshold T and amplitude threshold M that we tested. Setting $M = 10\sigma$ corresponds to a threshold of 1.9 nT for our full QF609 dataset associated with AR2007, very close to the threshold of 1.7 nT used by Bleier et al. (2009). Setting $M = 10\sigma$ and $T = 0$ s (i.e., no minimum duration) yielded pulse counts on QF609 with similar background numbers per day (zero to 15) as reported by Bleier et al. (2009). Absolute pulse counts are very dependent on the details of the algorithm (temporal threshold T and amplitude threshold $M\sigma$), but in a very non-linear way (Table 3), so changes in pulse rate are also likely sensitive to the precise details of the algorithm. We explore this sensitivity more in section 6 below. For the rest of this paper we report pulse counts using "$M=10\sigma$, $T=0$ s" (Figs. 7-11) and for comparison purposes report and show pulse counts using "$M=20\sigma$, $T=0$ s" in Supplementary Materials.

4.3.2 Alum Rock 10/31/2007 earthquake (AR2007)

We see an increase in pulse counts and a peak in pulse counts 13 days before the AR2007 earthquake as reported by Bleier et al. (2009) both for $M=10\ \sigma$, $T=0$ s (Fig. 7a) and for $M=20\ \sigma$, $T=0$ s (Fig. S5a). We examined the pulse counts for 9 months before and 6 months following AR2007 (excluding data gaps and known noise, Table S1; Fig. 5), to check for long-term changes and to confirm that this is an isolated event for QF609 near the time of the earthquake. Within the 15-month period examined, the increase in pulse counts prior to the Alum Rock earthquake is the most notable event: most days range from 5 to 25 pulses per day but the days before the earthquake increase to 70 to 150 pulses per day.

In contrast to QF609, pulse counts at JRSC and FRN do not show any visible features or trends related to the Alum Rock earthquake (Figs. 7b and c, S5b and c). This is consistent either with tectonic (earthquake-related) pulses occurring near QF609 but attenuated beyond detection at JRSC and FRN, or with the pulses at QF609 being non-tectonic from an as yet unknown cause (e.g., geomagnetic; or lightning; or cultural or instrumental artifacts). We also applied the same pulse-counting methodology to the vertical and north-south magnetometers at QF609 (Fig. S6).

Table 3: Average pulse counts per day for the 387 days around AR2007 (Table S1), and for the two weeks prior to AR2007 (10/15–10/30/2007), for different amplitude (M) and temporal (T) thresholds.

		All 387 days			**Two weeks prior to AR2007**		
T (s)	**M (σ)**	**QF609**	**JRSC**	**QF609 - JRSC**	**QF609**	**JRSC**	**QF609 - JRSC**
0	20	4	1	3	26	0	26
1	20	3	0	3	17	0	17
2	20	2	0	2	15	0	15
4	20	2	0	2	11	0	11
0	10	8	2	6	49	1	48
1	10	5	1	4	29	1	28
2	10	5	1	4	26	1	25
4	10	4	1	3	21	1	20
0	2	350	3000	-2650	650	1500	-850
0	6	24	23	1	69	19	50
* 0	10	8	2	6	49	1	48
0	14	6	1	5	36	0	36
* 0	20	4	1	3	26	0	26

*These two lines in the table are repeated from earlier in the Table to allow easier comparison of results.

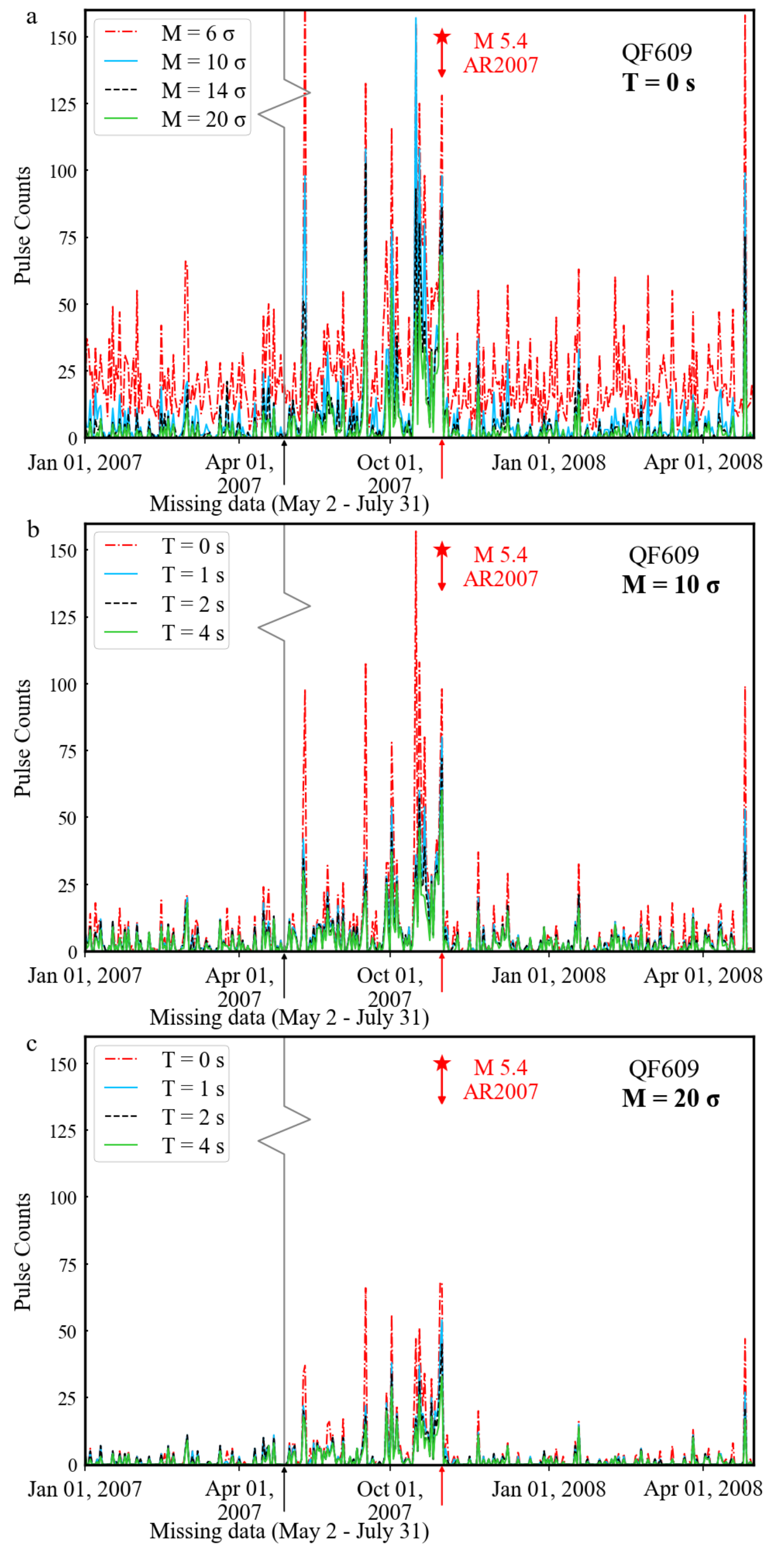

Figure 6: Effects of varying parameters on pulse counts for QF609 east-west magnetic coil for 2007–2008. (a) Pulse counts for different thresholds M, with T=0 s. (b) Pulse counts for varying duration parameter T, with M=10. (c) Pulse counts for varying T, with M=20.

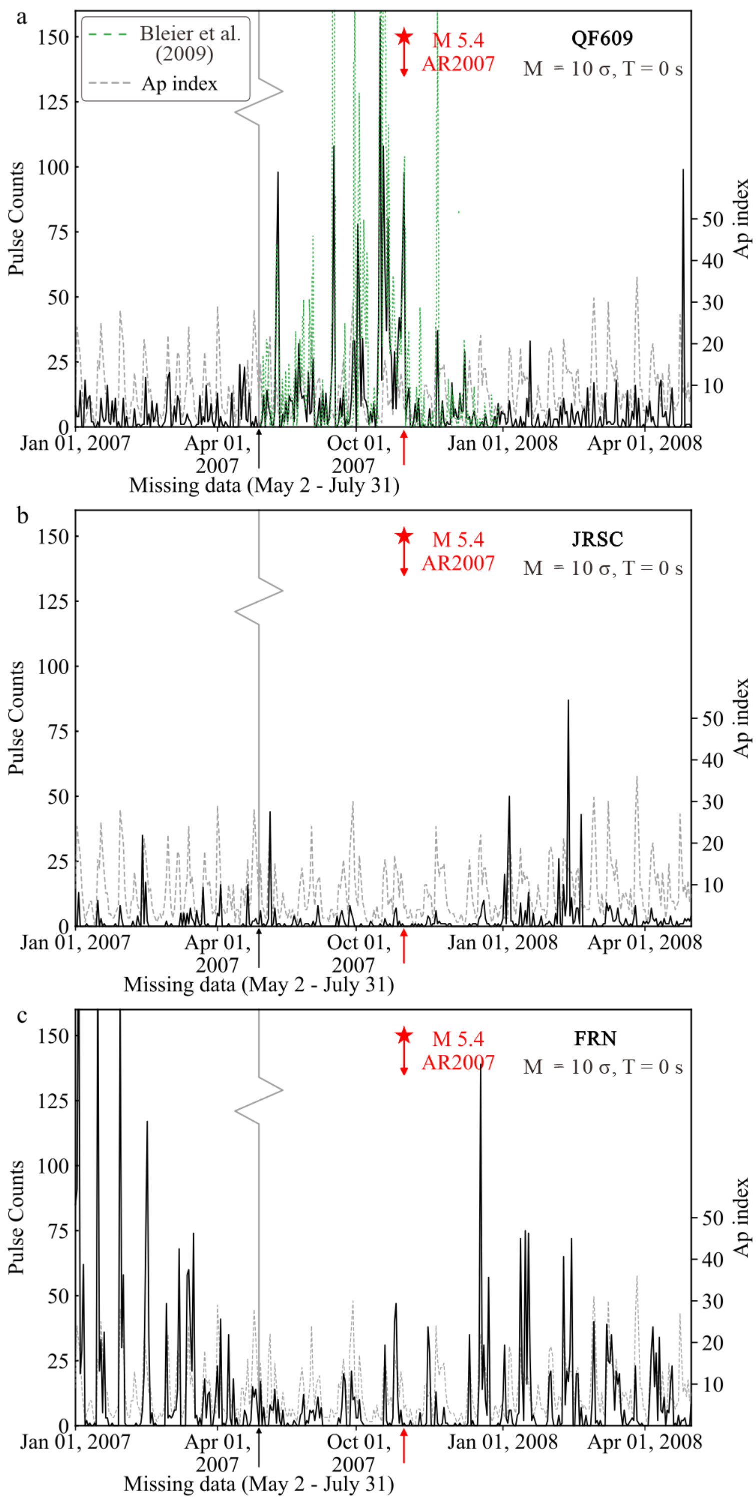

Figure 7: Pulse counts on east-west magnetic channels before and after AR2007, January 1, 2007 to April 30, 2008, made with M=10 σ, T=0 s. (a) QF609; (b) JRSC; (c) FRN. Dashed green lines in part a is the pulse counts for QF609 reported by Bleier et al. (2009). Gray dashed line: Ap index. Red line and star: AR2007 earthquake. (For equivalent Figs. with M=20 σ, T=0 s see Fig. S5).

4.3.3 Alum Rock 01/07/2010 earthquake (AR2010)

Dunson et al. (2011) reported pulse-count increases before the smaller (M4.0) 2010 Alum Rock earthquake, noting, however, that the increase in counts leading up to the smaller earthquake is smaller than in the larger (M5.4) AR2007 event. Using the same pulse-counting algorithm described in Section 4.3.1, we attempt to reproduce Dunson et al. (2011) results for pulse counts before and after the AR2010 earthquake (their Fig. 6), from March 19, 2009 through September 23, 2010 (as with AR2007 some days could not be examined, Table S1, Fig. S1).

Our pulse counts of QF609 data around AR2010 show the pulse count increase before the earthquake reported by Dunson et al. (2011) both for M=10σ, T=0 s (Fig. 8a) and for M=20σ, T=0 s (Fig. S7a). However, we do not consider this increase anomalous, as we find another, larger, pulse count increase in March 2010, 2.5 months after AR2010, that is not associated with any large earthquake event in the area, nor with anomalous geomagnetic activity (no increase in Ap index) (Fig. 8a), and a similar but smaller increased pulse count using M=20σ, T=0 s thresholds (Fig. S7a). In contrast, Dunson et al. (2011, their Fig. 6) show no daily pulse counts that are larger than 50% of their pre-earthquake spike in the months after AR2010, though they do show (their Fig. 17) at least one day on which the average pulse amplitude exceeded the pre-earthquake average pulse amplitude. The difference between our pulse counts and those of Dunson et al. (2011) strongly suggests an excessive sensitivity of these pulse counts to the pulse counting algorithm in use.

At JRSC all the days with the highest pulse counts are for dates after AR2010 (Fig. 8b, Fig. S7b), and we cannot discern any visible increases or other identifiable patterns related to AR2010, as expected from our results from the significantly larger event AR2007.

447 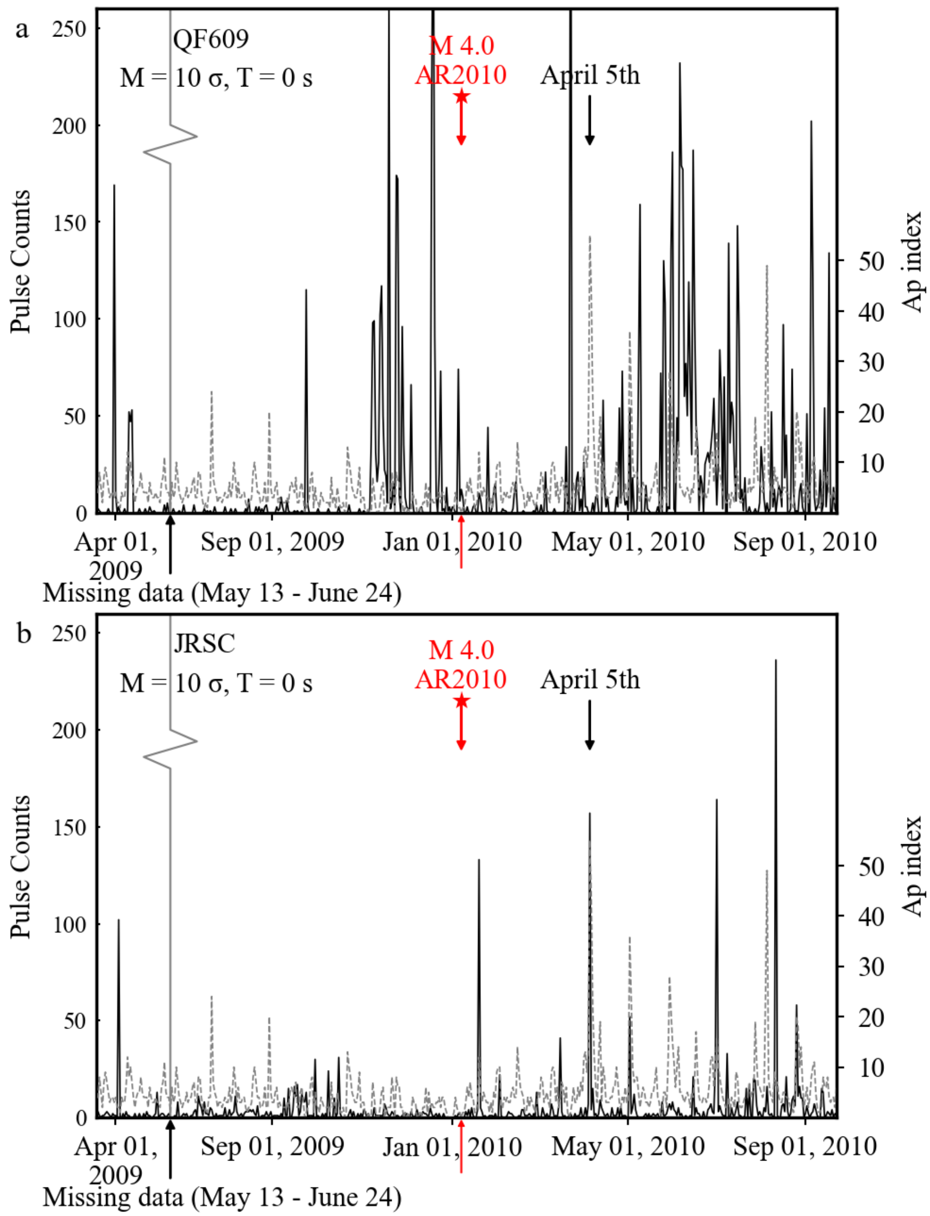

448 Figure 8: Pulse counts on east-west magnetic channels before and after AR2010, March 19, 2009
449 to September 24, 2010, made with M=10 σ, T=0 s. (a) QF609; (b) JRSC. Gray dashed line: Ap
450 index. Red line and star: AR2010 earthquake. (For equivalent figures with M=20 σ, T=0 s see
451 Fig. S7).
452

453 **4.3.4 Statistical Analysis**

454 We next briefly examine the statistics of the time variability of the pulse counts. To test
455 the statistical significance of the increase in pulse counts before the AR2007 event we initially
456 assume that the temporal distribution of pulses is a random, Poisson process (a distribution often

used to model earthquake main-shock occurrence, e.g., Gardner & Knopoff (1974)), although we cannot exclude other distributions (e.g., Dunson et al. (2011) speculate that pulses may follow a Weibull distribution). We compare the average pulse rate over the entire period studied (Table 3) to the rate of occurrence of pulses at times close to or long separated from the Alum Rock earthquakes, and the Poisson probability of such increased or diminished rates (Table 4).

Poisson distribution probability tells us that if we expect some independent event to occur λ times over a specified time interval then the probability P of exactly x occurrences is equal to,

$$P(x,\lambda) = \frac{\lambda^x\, e^{-\lambda}}{x!} \quad \text{(e.g., Boas, 1983)} \qquad (1)$$

where λ, our expected number of pulse counts for each time period considered, is based on the average over the entire period studied (387 days around AR2007, Table 4, and 502 days around AR2010, Table S4). x is the observed number of pulses over the shorter period in question, e.g., the 7 days in the week preceding the earthquake. Occurrence of pulse counts with probabilities lower than 0.05 are regarded as statistically significant if the underlying assumptions are correct (McKillup, 2006).

We see that the increase in average pulse counts starting two months before the 2007 Alum Rock earthquake on QF609 data, is statistically very significant when pulse counting both with M=10σ, T=0 s (Table 4) and also for M=20σ, T=0 s (Table S3). In contrast, there is no statistically significant change in average pulse counts on JRSC data before or after the 2007 Alum Rock earthquake. The statistically significant increases in pulse counts at QF609 before the AR2007 earthquake (and AR2010 earthquake, Table S4) could be indicative of a relationship between the increased pulse counts and the impending earthquake, or of some unknown anthropogenic effect.

However, caution is required, both because different patterns are seen around each earthquake, and because statistically improbable pulse counts are seen at times far removed from the earthquakes. Although in both 2007 and 2010 statistically significant increases in pulse counts were seen two months prior to the earthquake, for AR2007 the significant increases continue until the day of the earthquake itself, whereas for AR2010 there were statistically significant decreases in pulse rate the week before and on the day of the earthquake (Table 4, Table S4). Perhaps the simplest explanation is that the pulses – whether earthquake-related or anthropogenic – represent a highly clustered, non-Poissonian, distribution, as is the case for earthquake catalogues before removal of aftershock sequences (Gardner & Knopoff, 1974). This would explain how we could observe the occurrence of "one-in-a-million" event (≥22 pulses/day) on 32 out of 387 days around AR2007.

Without knowing the statistical characteristics of the pulse process, we cannot know whether the clear increase in pulse counts before the AR2007 earthquake (and on other specific days in the data) has any statistical significance.

Table 4: Pulses/day (counted with M=10σ, T=0 s) for various time periods associated with AR2007, for QF609 and JRSC.

Time period	**# of days**	**QF609,** pulses/day	**Probability of QF609**	**JRSC,** pulses/day	**Probability of JRSC**
All days (λ)	387	8		2	
EQ-8 months to EQ-2 months	147	6	0.12	2	0.27
EQ-2 months to EQ	60	23	7.66×10^{-6}	1	0.27
EQ-1 month to EQ	31	33	2.45×10^{-11}	1	0.27
EQ-1 week to EQ	8	31	4.04×10^{-10}	2	0.27
EQ day	1	68	3.48×10^{-39}	1	0.27
EQ+1 month to EQ+6 months	149	5	0.09	4	0.09

5 Testing alternate causes for pulses

We have shown that there is an apparent increase in the number of pulses before the AR2007 earthquake (Section 4.3.2) but that statistical tests of its relationship to the earthquake cannot be conclusive (Section 4.3.4). We have also shown that even with two stations, the amplitudes of the pulses do not conclusively discriminate between tectonic and non-tectonic origin (Section 4.2). Next, we consider other characteristics of the pulse series (temporal distribution) and the pulses (pulse length) that may help us to understand their causes.

5.1 Short-term temporal variation of pulse rate

To assess whether the pulses could be of external (ionospheric/magnetospheric) origin, we compared our pulse counts to the Ap geomagnetic index, a standard quantification of daily global geomagnetic activity on a scale from 0 to 400 (NOAA, 2014). Although a few pulse peaks coincide with increased Ap index (e,g, Fig. 8b, JRSC, April 5^{th} 2010) these may be coincidental and the lack of consistent visual correlation at either QF609 or JRSC (Figs. 7 and 8) suggests that geomagnetic storms are not a significant cause of the pulses at QF609. We note that if the pulses were external in origin then we would expect the same pulse pattern to appear at QF609 and JRSC (which is not the case for the April 5^{th} example flagged above, compare Figs. 8a and b, April 5^{th} 2010).

We next studied the daily distribution of pulses. Our null hypothesis is that tectonic pulses associated with earthquake activity are distributed randomly across the day, because tidal modulation of seismicity rates is very weak (a few %: Hao et al., 2018) and often hard to distinguish from periodic variation in signal detectability due to cyclical noise levels (Atef et al., 2009) except in the special case of magmatic earthquakes (e.g., Petrosino et al., 2018). Anthropogenic magnetic noise presumably peaks during working hours, while the BART electric train produces noise throughout the day except during approximately 02:00-04:00 clock time. In contrast, the local geomagnetic field is enhanced during daylight hours, showing a distinct increase in the two hours following local sunrise (e.g., Saka et al., 1982; Sentman & Fraser, 1991; Zomer et al., 2008), leading to increased noise activity. Similarly, lightning is not uniformly distributed through the day, but is concentrated in the late afternoon local time (solar time) in equatorial regions that host the majority of global lightning activity (Sentman & Fraser, 1991; Pan et al., 2013), largely corresponding to daylight hours in California. Over North America, more local to our array, the largest maximum of lightning activity is at about 18:00 local time, with a broader secondary peak between 11:00 and 12:00 local time (Pan et al., 2013). Instrumental noise is harder to assess: it could be equally distributed across all hours, or it could be triggered by thermal transients due, for example, to direct sunshine.

To assess the daily distribution of pulses, we repeated our pulse counting by counting pulses in each 1-hr window, now using an amplitude threshold calculated for the entire data ensemble rather than for each hour separately (using clock time CT, i.e., Pacific Standard Time (PST) in winter months, and Daylight Savings Time (DST) in summer months), and summing the total number of pulses in that hour over the entire 387 days studied around the AR2007 earthquake (Fig. 9a, Fig. S8a). Clearly at both QF609 and JRSC pulse activity peaks during normal daylight and working hours (8am–5pm clock time) and there is a clear minimum when BART is inactive (2am–4am clock time), that is absent in FRN. Over the 387 days counted, a very significant proportion of pulses must be cultural, due to BART and other anthropogenic noise that is strongest during normal working hours, and/or the geomagnetic field enhancement well-known to occur at sunrise, remain somewhat elevated during daylight hours, and decrease at sunset (e.g. Saka et al., 1982; Zomer et al., 2008).

At QF609 we see the same effect measured only over the two weeks immediately preceding AR2007 (Fig. 9b). We also examined the 27 other two-week periods before and after AR2007 (Jan 7, 2007–April 8, 2008) and calculated their mean and standard deviation pulse counts by hour (Fig. 9b). All two-week periods show the BART signature (few or zero pulses from ~02:00–04:00), and it is clear that the large increase in pulse rates prior to AR2007 (Fig. 7a) is dominated by activity in daylight hours.

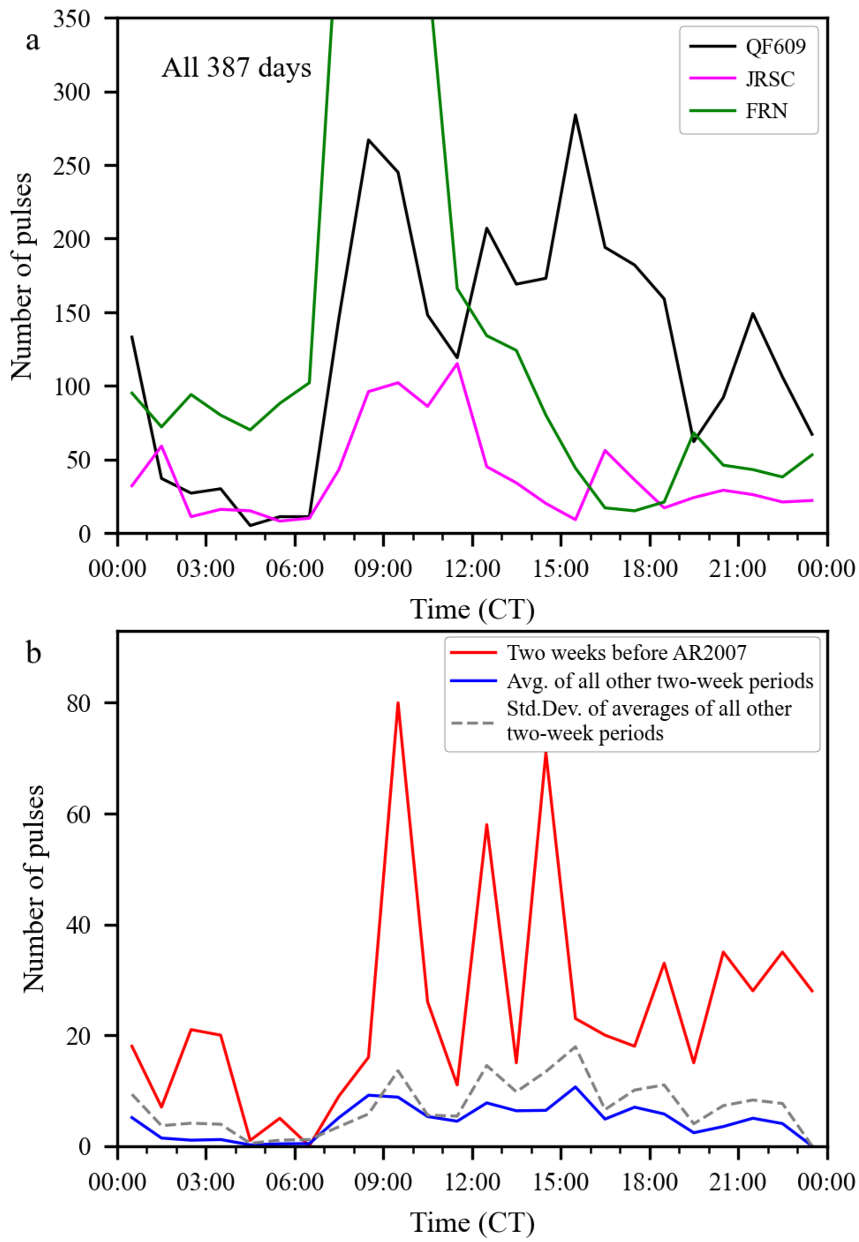

Figure 9: Pulse counts for QF609 from Fig. 7a (using M=10 σ, T=0 s) by hour of occurrence (clock time). (a) aggregated over all 387 days;(b) aggregated over just the two weeks immediately preceding AR2007 (red line) compared to average of pulse counts aggregated over all other two-week periods (blue line) and the standard deviation of these two-week aggregations (gray dashed line).

It is possible that there is a tectonic (precursory) increase in local conductivity that acts to amplify other external signals (cf. Merzer & Klemperer, 1997) so that the known diurnal behavior of BART is amplified, producing the excess of pulses in daylight hours. Additionally, other unknown and yet-to-be-recognized forces of precursory tectonic activity could lead to the increase in pulses during the day. However, if a significant proportion of the pulse increase preceding the AR2007 earthquake was tectonic, most hypotheses about precursory electromagnetic behavior would predict an increase in pulse counts at all hours of the day for these two weeks of enhanced activity, rather than having a clear minimum in the very early morning.

To emphasize this point, Fig. 10 compares the daily pulse count (made over a full 24 hours, as in Fig. 7) with the pulse count by day during the year only for pulses from 02:00-04:00 clock time. From 02:00–04:00: 1) BART is not running, 2) cultural activity should be minimized, 3) the sun has not risen with its consequent increase in magnetic activity, and 4) regional North American and global tropical lightning intensity is low. In Fig. 7 we made all pulse counts using a threshold based on the average of each daily standard deviation, irrespective of the hour at which each pulse occurred. In contrast, in Fig. 10 we used amplitude thresholds calculated separately either from the average of the standard deviations for each 24-hour period (for the total count each day over 24 hours, as in Figs. 7 and 9), or from the average of the standard deviations for just the two-hour quiet periods (for the total count within the quiet period per calendar day). Because pulses during this quiet time are counted above thresholds that are lower by a factor of ~3 compared to the average daily threshold (Table S2) there can be far higher pulse counts for a 02:00–04:00 two-hour period than for the whole day containing that two-hour period. Since, as we have shown, many pulses at both QF609 and JRSC are either cultural or related to diurnal variation in geomagnetic field or lightning, any changes in rates of occurrence of tectonic pulses should be more dramatic during the quiet period than when averaged over the whole day. For both QF609 and JRSC, we found the pulse count patterns before and after the AR2007 earthquake for the quiet hours were very different than for all hours of the day (Fig. 10). The increase in QF609 pulse counts leading up to the earthquake, measured during quiet hours, is only

586 present for a week before the earthquake, rather than a month when estimated across all 24 hours
587 (Fig. 10a), and a much larger increase in pulse rate is visible a week after AR2007.

588 We conclude that most, if not all, the pulses counted at QF609 and JRSC were unrelated
589 to tectonic sources.

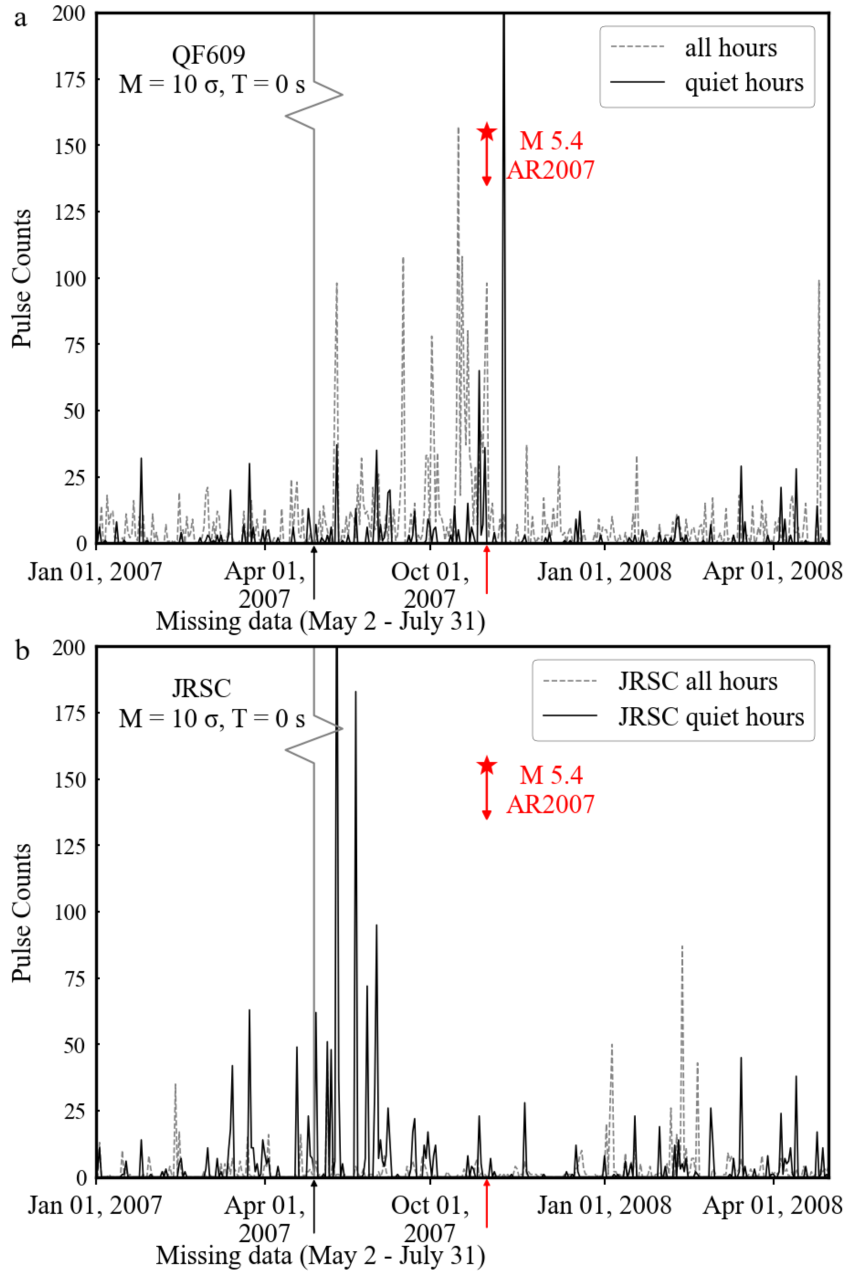

590

591 Figure 10: Pulse counts (using M=10 σ, T=0 s) by date for only 02:00–04:00 clock time (solid
592 lines) for (a) QF609 and (b) JRSC compared to 24-hour pulse counts (gray dashed lines) repeated
593 from Fig. 7a, b. For M=20 σ, T=0 s, see Fig. S10.

5.2 Distribution of pulse lengths

Because it is well known that lightning can induce magnetic pulses (e.g., Sentman & Fraser, 1991; Fraser-Smith & Kjono, 2014), Bleier et al. (2009) attempted to correlate pulse occurrence at QF609 with local commercial lightning detections within California. Bleier et al. (2009) found that pulses generated by local (within a few hundred km of QF609) lightning are characteristically short, < 0.5 s. However, in principle, QuakeFinder and Stanford-USGS magnetometers are capable of recording electromagnetic signals produced by lightning that occur anywhere in the world (e.g., Inan et al., 2010), and these signals can have periods exceeding 1 second (Rakov et al., 2007), although such long pulses are much less common than higher-frequency pulses (e.g., Fraser-Smith & Kjono, 2014).

Bleier et al. (2009) plotted the distribution of pulses of different T (the time for which a pulse exceeds the amplitude threshold) from 1 to 30 s, i.e., durations which exceed the pulse durations they expect from lightning, and the durations of various signals from cultural sources they tested. Bleier et al. (2009, their Fig. 10) showed that the rate of pulses decreases dramatically with increasing pulse duration, but they did not more closely characterize the distribution. We therefore extended this analysis to shorter T, and in Fig. 11 we plot log number of pulses against log reciprocal duration. Our number of pulses is a proxy for amplitude of the geomagnetic field, while our reciprocal duration is a proxy for frequency. Because our method measures a pulse as short-duration if it very briefly exceeds the amplitude threshold, even if it is actually a very long-period signal, we cannot directly convert our measured durations that span 0.1–20 s to frequencies of 0.025–5.0 Hz. However, to the extent that our measured pulse durations correspond to reciprocal frequency f, both QF609 and JRSC show log number of pulses increasing with $\sim f^{+1}$ over this bandwidth. This positive slope in Fig. 11 is opposite to the well-known amplitude spectrum of the external geomagnetic field that decreases as f^{-1} to $f^{-1.5}$ in this part of the spectrum (Lanzerotti et al., 1990). The positive slope of Fig. 11 is also opposite to the expected $f^{-0.5}$ variation in signal amplitude for electromagnetic signals originating at constant depth in the earth, due to attenuation (the skin depth effect). Thus – with the caveat that pulse length may be a poor proxy for pulse frequency – the very large number of short pulses compared to longer durations seems to rule out both external geomagnetic sources and tectonic signals from a fixed (hypocentral?) depth as a cause for most counted pulses. The amplitude spectrum of BART signals also decreases with increasing frequency as $\sim f^{-2}$ (Fraser-Smith & Coates, 1978). Hence the most likely cause of the counted pulses appears to be local instrumental or cultural sources, but not BART, at both QF609 and JRSC.

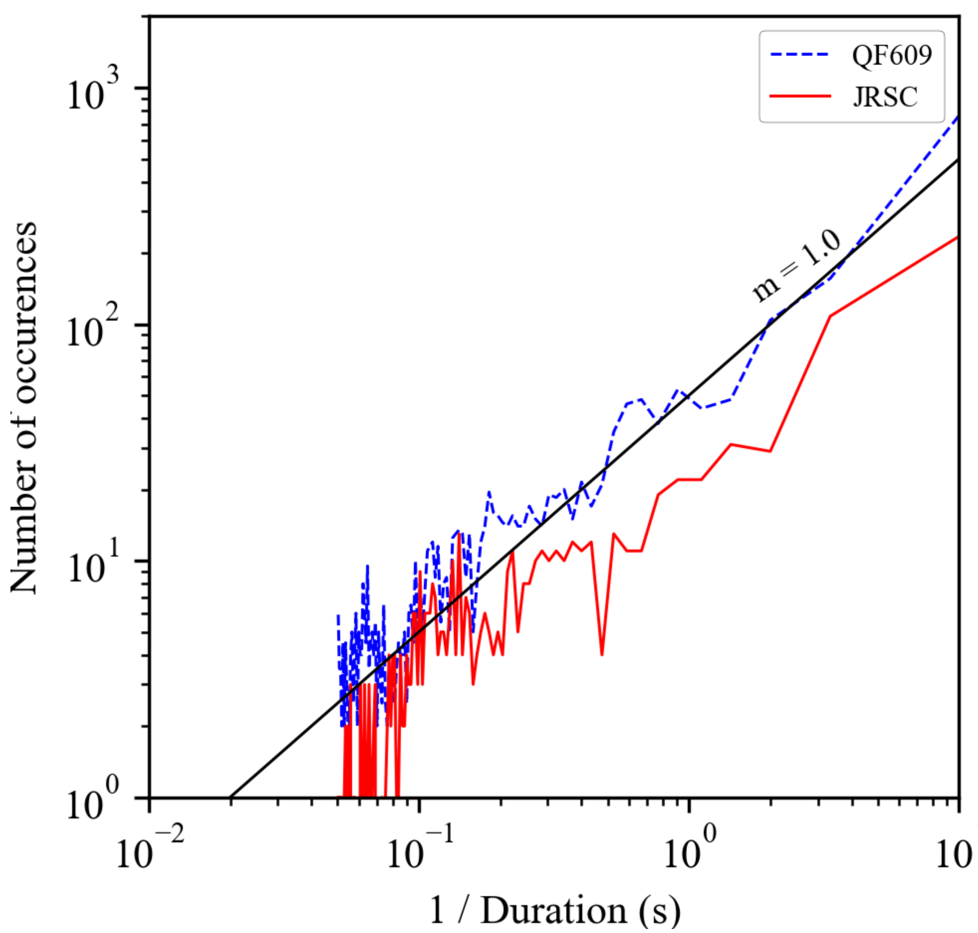

Figure 11: Log number of pulses of specific duration (counted with M=10 σ, T=0) aggregated over all 387 days counted around AR2007 event, plotted against log (reciprocal duration/second), calculated for 0.1 second durations from 0.1–20 s, plotted at bin centers. Dashed blue line: QF609. Solid red line: JRSC For M=20 σ, T=0 s see Fig. S12.

6 Importance of parameter selection for pulse-counting algorithms

Any study attempting to recognize tectonic magnetic pulses is greatly hampered by uncertainty about the physical mechanism that might create magnetic pulses. We lack the physical basis for selecting the parameters of our pulse-counting algorithm, and we cannot assess whether the observed variability in pulse rates is statistically significant. Nonetheless, our results may suggest appropriate strategies for pulse-counting, and also offer insights into possible pulse mechanisms. We described (above) how changing different parameters of the pulse counting algorithm affects the results (Table 3, Fig. 6). Changing our amplitude threshold $M\sigma$ changes the number of pulses counted, but varying $M\sigma$ within the ranges shown does not affect the observed increase in pulse count prior to the 2007 Alum Rock earthquake (Fig. 6a). Thus our relatively simple pulse counter is reasonably robust to parameter choices. Dunson et al. (2011) used a more complex pulse counter that focuses only on unipolar pulses, so that reducing the amplitude threshold not only counts more small pulses, but also excludes some larger pulses that are unipolar when tested against a high threshold, but become bipolar when tested against a low threshold. Dunson et al. (2011, their Figs. 6 and 7) showed that reducing the amplitude threshold by a factor of 2.5 removes the increase in pulse counts observed by Bleier et al. (2009) prior to the AR2007 event. In the absence of an established physical mechanism, we do not consider a more complex pulse counter to be warranted.

Although all values of amplitude threshold $M\sigma$ for fixed temporal threshold $T = 0$ s show the increase in pulse counts prior to the AR2007 earthquake at QF609, and no increase at JRSC, we do see that the data recorded at the two stations has different characteristics. Table 3 shows the difference in average pulse counts per day between QF609 and JRSC. For most thresholds tested, QF609 records more pulses than JRSC; but for the lowest amplitude threshold $M = 2$, JRSC records vastly more pulses than QF609. This reinforces our belief that QF609 is recording (at least in part) a different class of signals from those seen at JRSC, whether anthropogenic or otherwise, including a proportionally greater number of the highest amplitude pulses. We next explore these differences further by looking at the temporal threshold T.

In our pulse counter, in order for a signal to be counted as a pulse, it must exceed the amplitude threshold for a time period greater than the minimum duration T. Changing our temporal threshold T from 0 to 4 s changes the number of pulses counted (Table 3), and the anomalous increase in pulse counts 13 days before the AR2007 earthquake in QF609 data gradually decreases as T is increased. For our chosen amplitude threshold M=10, the pulse counts – whether for all 387 days or just the 13 days before AR2007 –show that QF609 averaged ~2 times as many pulses per day with zero temporal threshold compared to T = 4 s. Thus, even though Bleier et al. (2009) found numerous pulses with time duration exceeding a few seconds, it is clear that the rate of these longer period pulses does not increase prior to the earthquake; rather it is the number of shorter-period pulses that increases slightly prior to the earthquake. Changing T for the JRSC data gradually decreases the pulse counts each day but does not change the overall pattern (Fig. S4b). There is no T that results in an increase in pulses before the earthquake on JRSC.

7 DISCUSSIONS AND CONCLUSIONS

We corroborate the reported increase in pulsations before the AR2007 earthquake as reported by Bleier et al. (2009) at QF609 but were unable to identify a precursory signal at the next-nearest station, JRSC, located four times farther away from the hypocenter. We were unable to corroborate an increase at QF609 or JRSC before the AR2010 earthquake. To date, no study has yet confirmed a magnetic earthquake precursor at two separate stations.

If tectonic pulses exist, the simplest model is for their occurrence to be uniformly distributed throughout the day, with no bearing on cultural activity. However, when we look at the daily distribution of pulses, we see that the majority of pulses occur during culturally active times. Looking specifically at quiet times of the day (2am-4am clock time), there was no increase in pulse counts before AR2007. This indicates that the pulses are cultural in origin. As yet there is no reliable indication from observation or theory that tectonic processes generate ULFEM pulses. We speculate that if tectonic pulses exist, they should have the greatest occurrence or magnitude during the earthquake, associated with the largest release of energy. However, the largest increase in pulse counts or magnitude of pulses is not observed during the earthquake. If tectonic pulses do exist, it is clear from the analyses presented here, identifying them will require availability of an appropriate regional reference observatory to reduce ionospheric and magnetospheric disturbances and a network of stations that are not located near sources of cultural noise.

Although in some respects the patterns of pulse counts are robust and do not depend on the characteristics of the pulse-counting algorithm, in other respects the patterns are sensitive to arbitrarily chosen conditions and parameters (Fig. 6). This may indicate that at the present state of knowledge, with speculations but no widely accepted theory for tectonic generation of pulses (e.g., Bleier et al., 2009), it is premature to focus on pulses as reflecting pre-earthquake anomalies. Given the clear cultural signal in the pulse distribution, and the lack of a precursory increase in pulse counts seen during quiet times, we conclude that the pulse increase before the Alum Rock 2007 earthquake has no tectonic significance.

Studies of pulsations potentially associated with earthquakes 1) need to verify the robustness of the pulse detection algorithm; 2) should attempt to incorporate adaptive filtering to isolate ionospheric and magnetospheric signals, and 3) must continue to pay careful attention to the possibility of unrecognized anthropogenic signals. No single test – whether statistical over months/years, or day/night variation, or frequency content, or relative amplitude at different sites – is sufficient to identify the origin of the pulses. Multiple tests using multiple stations that are located within distances sufficient to distinguish tectonic signals are required to be able to properly assess whether tectonic electromagnetic signals occur, in addition to distinguishing between anthropogenic contamination and naturally occurring solar/ionospheric/atmospheric geomagnetic fluctuations. As a result, we encourage future researchers to take a broader view of the ULF band.

9 ACKNOWLEDGEMENTS

We are grateful to QuakeFinder for providing access to their full data set from QF609, and to Clark Dunson and Tom Bleier who comprehensively described their pulse-counting software and their understanding of their data-sets and possible sources of the pulses. We thank Malcolm Johnston for comments and discussions on early versions of this manuscript. QuakeFinder data acquisition was funded by Stellar Solutions Inc. with supplemental funding by NASA Grant NNX12AQ05A. Jared Peacock consulted on possible signal scaling and efficient script writing. The Stanford-USGS ULFEM network was funded by NASA contract NHH08AH44I to JG and NSF grant EAR-0346236 to SLK. This research was supported by the USGS and Stanford University, and by UC Berkeley which archives the JRSC data, and from whom the raw data may be obtained. Any use of trade, firm, or product names is for descriptive purposes only and does not imply endorsement by the U.S. Government.

10 DATA AVAILABILITY

The QuakeFinder magnetic data are available from Quakefinder and Stellar Solutions Inc.; the Stanford-USGS data are available either from the Stanford or from the USGS.

11 REFERENCES

Atef, A.H., Liu, K.H. & Gao, S.S., 2009. Apparent Weekly and Daily Earthquake Periodicities in the Western United States. *Bull. Seismolog. Soc. Am.*, **99,** 2273-2279.

Bedrosian, P.A., Unsworth, M.J. & Egbert, G., 2002. Magnetotelluric imaging of the creeping segment of the San Andreas Fault near Hollister, *Geophysical Research Letters,* **29(11)**, 1.1-1.4.

Bijoor, S., Glen, J., McPhee, D.K. & Klemperer, S.L., 2005. Ultra-low frequency electromagnetic monitoring of earthquakes in the San Francisco Bay Area: initial results of an Earthscope PBO Project, *EOS Trans., AGU*, **86 (52)**, Fall Meet. Suppl., Abstract T51B-1343, and https://pangea.stanford.edu/researchgroups/crustal/sites/default/files/Bijoor.ULFEMmonitoring.AGUposter.2005.pdf

Bleier, T., Dunson, C., Maniscalco, M., Bryant, N., Bambery, R. & Freund, F., 2009. Investigation of ULF magnetic pulsations, air conductivity changes, and infra-red signatures associated with the 30 October Alum Rock M5.4 earthquake, *Nat. Hazards Earth Syst. Sci.*, **9**, 585–603, doi:10.5194/nhess-9-585-2009.

Boas, M., 1983. *Mathematical methods in physical sciences*, 2nd ed., 729, John Wiley & Sons.

Campbell, W. H., 2009. Natural magnetic disturbance fields, not precursors, preceding the Loma Prieta earthquake, *Journal of Geophysical Research: Space Physics (1978–2012)*, **114(A5)**, doi:10.1029/2008JA013932.

Cicerone, R.D., Ebel, J.E. & Britton, J., 2009. A systematic compilation of earthquake precursors, *Tectonophysics*, **476**, 371–396, doi:10.1016/j.tecto.2009.06.008.

Culp, D., Klemperer, S., Glen, J. & McPhee, D., 2007. Re-affirming the Magnetic Precursor to the 1989 Loma Prieta, CA, Earthquake Using Magnetic Field Data Collected in the US in 1989 and 1990, *EOS Trans., AGU*, **87**, Abstract S41D-03, http://www.agu.org/meetings/fm07/fm07-sessions/fm07_S41D.html and https://pangea.stanford.edu/researchgroups/crustal/sites/default/files/CulpKlemperer.LomaPrieta.AGUtalk.2007_0.pdf

Cutler, J., Bortnik, J., Dunson, C., Doering, J., & Bleier, T., 2008. CalMagNet - an array of search coil magnetometers monitoring ultra-low frequency activity in California, *Natural Hazards and Earth System Science*, **8(2)**, 359-368.

Davis, P.M., and Johnston, M.J.S., 1980. Further evidence of localized geomagnetic field changes before the 1974 Thanksgiving Day earthquake, Hollister, California: Geophysical Research Letters, 7, 513-517.

Davis, P.M., and Johnston, M.J.S., 1983. Localized geomagnetic field changes near active faults in California 1974-1980: Journal of Geophysical Research, 88, 9452-9460.

Dunson, J. C., Bleier, T. E., Roth, S., Heraud, J., Alvarez, C. H. & Lira, A., 2011. The Pulse Azimuth effect as seen in induction coil magnetometers located in California and Peru 2007--2010, and its possible association with earthquakes, *Natural Hazards & Earth System Sciences*, **11**, 2085-2105.

Eberhart-Phillips, D., Labson, V.F., Stanley, W.D., Michael, A.J. & Rodriguez, B.D., 1990. Preliminary velocity and resistivity models of the Loma Prieta earthquake region, *Geophysical Research Letters*,17(8), 1235-1238.

Fenoglio, M. A., Fraser-Smith, A. C., Beroza, G. C. & Johnston, M. J. S., 1993. Comparison of ultra-low frequency electromagnetic signals with aftershock activity during the 1989 Loma Prieta earthquake sequence, *Bulletin of the Seismological Society of America*, **83(2)**, 347-357.

Fraser-Smith, A. C. & Coates, D. B., 1978. Large-amplitude ULF electromagnetic fields from BART, *Radio Science*, **13**, 661-668.

Fraser-Smith, A. C. & Kjono, S.N., 2014. The ULF magnetic fields generated by thunderstorms: A source of ULF geomagnetic pulsations?, *Radio Sci.*, **49**, doi:10.1002/2014RS005566.

Fraser-Smith, A. C., McGill, P. R. & Bernardi, A., 2011. Comment on “Natural magnetic disturbance fields, not precursors, preceding the Loma Prieta earthquake” by Wallace H. Campbell, *Journal of Geophysical Research: Space Physics (1978–2012)*, **116(A8)**, doi:10.1029/2010JA016379.

Fraser-Smith, A.C., Bernardi, A., McGill, P.R., Ladd, M.E., Helliwell, R.A. & Villard, O.G., Jr., 1990. Low-frequency magnetic field measurements near the epicenter of the Ms 7.1 Loma Prieta earthquake, *Geophys. Res. Letts*, **17**, 1465-1468.

Fraser-Smith, A.C., McPhee, D.K., Glen, J.M., Klemperer, S.L., McGill, P.R. & Bernardi, A., 2013. Comments on "On the reported magnetic precursor of the 1989 Loma Prieta earthquake" by J. N. Thomas, J. J. Love, & M. J. S. Johnston, https://pangea.stanford.edu/researchgroups/crustal/sites/default/files/FraserSmithetal.CommentonThomas09.PEPIsubmitted.pdf, EarthArXiv, https://doi.org/10.31223/X5JK54

Gardner, J.K. & Knopoff, L., 1974. Is the sequence of earthquakes in Southern California, with aftershocks removed, Poissonian?, *Bulletin of the Seismological Society of America*, 64.

Hao, J., Zhang, J., & Yao, Z., 2019. Evidence for diurnal periodicity of earthquakes from midnight to daybreak. *National Science Review*, **6,** 1016-1023.

Hayakawa, M., Kawate, R., Molchanov, O. A. & Yumoto, K., 1996. Results of ultra-low frequency magnetic field measurements during the Guam earthquake of 8 August 1993, *Geophys. Res. Letts.* **23**, 241-244.

Inan, U. S., Cummer, S. A. & Marshall, R. A., 2010. A survey of ELF and VLF research on lightning-ionosphere interactions and causative discharges, *J. Geophys. Res.*,**115**, A00E36, doi:10.1029/2009JA014775.

Johnston, M.J.S., Mueller, R.J., Ware, R., and Davis, P.M., 1984. Precision of magnetic measurements in a tectonically active region: Journal of Geomagnetism and Geoelectricity, 36, 83-95.

Johnston, M.J.S, 1998. Review of Electrical and Magnetic Fields Accompanying Seismic and Volcanic Activity, Surv. in Geophys., 18, 441-475.

Johnston, M.J.S., Y. Sasai, G.D. Egbert and R.J. Mueller, 2006. Seismomagnetic Effects from the long-awaited September 28, 2004, M6 Parkfield Earthquake. Bull. Seis. Soc. Am., 96, 206-220.

Karakelian, D., Klemperer, S.L., Fraser-Smith, A.C., & Beroza, G.C., 2000. A transportable system for monitoring ultra-low frequency electromagnetic signals associated with earthquakes, *Seismological Research Letters*, **71**, 423-436.

Karakelian, D., Beroza, G. C., Klemperer, S., Fraser-Smith, A. C., 2002. Analysis of ultralow-frequency electromagnetic field measurements associated with the 1999 M7.1 Hector Mine, California, earthquake sequence, Bull. Seis. Soc. Am. 92, 1513-1524.

Kolář, P., 2010. Some possible correlations between electro-magnetic emission and seismic activity during West Bohemia 2008 earthquake swarm, *Solid Earth*, ***1(1)***, 93-98.

Kopytenko, Yu.A., Matiashvili, T.G., Voronov, P.M., Kopytenko, E.A. and Molchanov, O.A. 1993. Detection of ultra-low frequency emissions connected with the Spitak earthquake and its aftershock activity, based on geomagnetic pulsations data at Dusheti and Vardzia observatories, *Phys. Earth Planet. Int.*, **77**, 85-95.

Lanzerotti, L. J., Maclennan, C. G. & Fraser-Smith, A. C., 1990. Background magnetic spectra:∼ 10− 5 to∼ 105 Hz, *Geophysical Research Letters*, **17(10)**, 1593-1596.

Li, M., Lu, J., Parrot, M., Tan, H., Chang, Y., Zhang, X. & Wang, Y., 2013. Review of unprecedented ULF electromagnetic anomalous emissions possibly related to the Wenchuan Ms= 8.0 earthquake, on 12 May 2008, *Natural Hazards & Earth System Sciences*, **13(2),** 279-286.

Liu, J.Y., Chen, C.H., Chen, Y.I., Yen, H.Y., Hattori, K. & Yumoto, K., 2006. Seismo-geomagnetic anomalies and M ≥5.0 earthquakes observed in Taiwan during 1988-2001, *Physics and Chemistry of the Earth 31*, 215-222.

Liu, T. T. & Fraser-Smith, A. C., 1996. Hayward Fault Earthquake Prediction Project: ULF magnetic field measurements, *Final Report*, *EPRI Project #WO8035-02*, Space, Telecommunications and Radio science Lab., Stanford University, December 1996.

Masci, F., 2011. On the seismogenic increase of the ratio of the ULF geomagnetic field components, *Physics of the Earth and Planetary Interiors*, **187(1)**, 19-32.

Masci, F., Palangio, P. & Di Persio, M., 2009. Magnetic anomalies possibly linked to local low seismicity, *Natural Hazards and Earth System Sciences*, **9**, 1567-1572.

McKillup, S., 2006. Probability helps you make a decision about your results, in *Statistics Explained: An Introductory Guide to Life Scientists (1st edn.)*, **44-56**, Cambridge University Press.

Merzer, M. & Klemperer, S.L., 1997. Modeling low-frequency magnetic-field precursors to the Loma Prieta earthquake with a precursory increase in fault-zone conductivity, *Pure and Applied Geophysics*, **150(2)**, 217-248.

Mueller, R.J., and Johnston, M.J.S., 1997. Magnetic Field Monitoring near Active Faults and Volcanic Caldera in California: 1974-1995, Phys. Earth. Planet. Int., 105, 131-144.

Neumann, D.A., McPherson, S.-L., Kappler, K., Klemperer, S., Glen, J. & McPhee, D., 2008. Stanford–USGS Ultra-Low Frequency Electromagnetic Network: Status report and data availability via the Web, *EOS Trans., AGU*, **88 (52)**, Fall Meet. Suppl., Abstract S53B-1824, and https://pangea.stanford.edu/researchgroups/crustal/sites/default/files/NeumannMcPherson.ULFEM_.AGUposter.2008.pdf

NOAA, 2014 http://www.ngdc.noaa.gov/stp/geomag/kp_ap.html

Pan, L., Liu, D., Qie, X., Wang, D. & Zhu, R., 2013) Land-sea contrast in the lightning diurnal variation as observed by the WWLLN and LIS/OTD data, *Acta Meteorologica Sinica*, **27**, 591-600.

Petrosino, S., Cusano, P., & Madonia, P., 2018. Tidal and hydrological periodicities of seismicity reveal new risk scenarios at Campi Flegrei caldera. *Sci. Rep.*, **8(1),** 1-12.

Rakov, V.A. & Uman, M.A., 2007. *Lightning: Physics and Effects*, Cambridge University Press.

Romanova, N.V., Pilipenko, V.A. & Stepanova, M.V., 2015. On the magnetic precursor of the Chilean Earthquake of February 27, 2010, Geomag. and Aeronomy, 55, 219-222.

Saka, O., Itonaga, M. & Kitamura, T., 1982. Ionospheric control of polarization of low-latitude geomagnetic micropulsations at sunrise, *Journal of Atmospheric and Terrestrial Physics*, **44(8)**, 703-712.

Sentman, D. D. & Fraser, B. J., 1991. Simultaneous observations of Schumann resonances in California and Australia: Evidence for intensity modulation by the local height of the D region, *Journal of Geophysical Research: Space Physics (1978–2012)*, **96(A9)**, 15973-15984.

Thomas, J. N., Love, J. J. & Johnston, M. J. S., 2007. The 1989 Ms 7.1 Loma Prieta, California, magnetic earthquake precursor revisited, *EOS Trans., AGU*, **87**, S41D-02. http://www.agu.org/meetings/fm07/fm07-sessions/fm07_S41D.html

Thomas, J. N., Love, J. J. & Johnston, M. J. S., 2009a. On the reported magnetic precursor of the 1989 Loma Prieta earthquake, *Phys. Earth Planet. Int.*, **173,** 207–215.

Thomas, J.N., Love, J.J., Johnston, M.J.S. & K. Yumoto 2009b. On the reported magnetic precursor of the 1993 Guam earthquake, Geophys. Res. Lett., 36, L16301, doi:10.1029/2009GL039020.

Thomas, J. N., Love, J. J. & Johnston, M. J. S., 2013. Comment on "On the reported magnetic precursor of the 1989 Loma Prieta earthquake" by J.N. Thomas, J.J. Love, and M.J.S. Johnston by A.C. Fraser-Smith, P.R. McGill, and A. Bernardi & Comment on "On the reported magnetic precursor of the 1989 Loma Prieta Earthquake" by J. N. Thomas, J. J. Love, and M. J. S. Johnston by J.M.G. Glen, S.L. Klemperer, and D.K. McPhee http://earthweb.ess.washington.edu/jnt/LomaPrieta/JNThomas_PEPI_Reply.pdf

Tsai, Y. B., Liu, J. Y., Ma, K. F., Yen, H.K., Chen, K.S., Chen, Y.I., and Lee, C.P., 2006. Precursory phenomena associated with the 1999 Chi-Chi earthquake in Taiwan as identified under the iSTEP program, *Physics and Chemistry of the Earth*, 31(4–9), 365–377.

Wang, C., Bin, C., Christman, L.E., Glen, J.M., Klemperer, S.L., McPhee, D.K., Kappler, K.N., Bleier, T.E. and Dunson, J.C., 2018. Cross-validation of independent ultra-low-frequency magnetic recording systems for active fault studies. *Earth, Planets and Space*, *70*(1), p.57.

Ware, R.H., Johnston, M.J.S., and Mueller, R.J., 1985. A comparison of proton and self-calibrating rubidium magnetometers for tectonomagnetic studies: *Journal of Geomagnetism and Geoelectricity*, **37,** 1051-1061.

Xu, G., Han, P., Huang, Q., Hattori, K., Febriani, F. & Yamaguchi, H., 2013. Anomalous behaviors of geomagnetic diurnal variations prior to the 2011 off the Pacific coast of Tohoku earthquake (Mw9. 0), Journal of Asian Earth Sciences, 77, 59-65.

Zomer, A., Price, C., Alperovich, L., Finkelstein, M. & Merzer, M., 2008. ULF amplitude observations at the dawn/dusk terminators, Journal of Atmospheric Electricity, 28(1), 21-29.

Supplementary Materials for:

Assessment of a claimed ultra-low frequency electromagnetic (ULFEM) earthquake precursor

Can Wang[1,2,3], Lilianna E. Christman[1,2], Simon L. Klemperer [2], Jonathan M. Glen [1], Darcy K. McPhee[4], Bin Chen [1,3]

[1]U.S. Geological Survey, Menlo Park, CA 94025, USA
[2]Department of Geophysics, Stanford University, CA 94305-2215, USA
[3]Institute of Geophysics, China Earthquake Administration, Beijing 100081, P.R. China
[4]U.S. Geological Survey, Reston, VA 20192, USA

These materials include Supplementary Tables S1 to S4; and Supplementary Figures S1 to S12.

Supplementary tables

Supplementary Table S1:
Days excluded from pulse counting before and after AR2007 and AR2010 earthquakes

Alum Rock 2007 Earthquake (10/31/2007): pulses were counted on all days January 1, 2007 – April 30, 2008, excluding:
March 14, 2007
April 4, 2007
April 20 - 21, 2007
April 24, 2007
May 2 - July 31, 2007
September 17, 2007
January 7 - 8, 2008

Alum Rock 2010 Earthquake (01/07/2007): pulses were counted on all days March 19, 2009 – September 24, 2010), excluding:
April 28 - May 1, 2009
May 13 - June 24, 2009
January 19, 2010
July 8, 2010
August 30 - 31, 2010
September 3, 2010

Supplementary Table S2:
Standard deviation for AR2007 and AR2010 earthquakes, calculated over all days, and either all hours or just quiet hours

	QF609 σ / nT	**JRSC σ / nT**
AR2007 All hours	0.19	0.13
AR2007 Quiet hours (02:00-04:00 clock time)	0.059	0.042
AR2010 All hours	0.54	0.10

Supplementary Table S3: Pulses/day (counted with M=20σ, T=0 s) for various time periods associated with AR2007, for QF609 and JRSC, and probability of that number of pulses occurring.

Time period	# of days	Pulses/day, QF609	Probability, QF609	Pulses/day, JRSC	Probability, JRSC
All days (λ)	387	4	N/A	1	N/A
EQ-8 to EQ-2 months	147	3	0.2	0	0.37
EQ-2 months to EQ	60	13	1.97×10^{-4}	0	0.37
EQ-1 month to EQ	31	19	4.14×10^{-8}	0	0.37
EQ-1 week to EQ	8	31	1.03×10^{-17}	0	0.37
EQ day	1	68	6.43×10^{-58}	0	0.37
EQ+1 to EQ+6 months	149	2	0.14	1	0.37

Supplementary Table S4:

Pulses/day (top, counted with M=10σ, T=0 s; bottom counted with M=20σ, T=0 s) for various time periods associated with AR2010, for QF609 and JRSC, and probability of that number of pulses occurring.

Time period M=10σ, T=0 s	# of days	Pulses/day, QF609	Probability, QF609	Pulses/day, JRSC	Probability, JRSC
All days (λ)	502	17	N/A	4	N/A
EQ-5 to EQ-2 months	180	3	3.39×10^{-5}	3	0.19
EQ-2 months to EQ	62	38	4.52×10^{-6}	1	0.07
EQ-1 month to EQ	32	27	6.34×10^{-3}	1	0.07
EQ-1 week to EQ	8	12	5.03×10^{-2}	1	0.07
EQ day	1	12	5.03×10^{-2}	0	0.02
EQ+1 to EQ+6 months	151	25	1.54×10^{-2}	5	0.16
M=20σ, T=0 s					
All days (λ)	502	11	N/A	1	N/A
EQ-5 to EQ-2 months	180	2	1.01×10^{-3}	1	0.36
EQ-2 months to EQ	62	27	2.01×10^{-5}	0	0.36
EQ-1 month to EQ	32	17	2.37×10^{-2}	0	0.36
EQ-1 week to EQ	8	9	1.08×10^{-1}	0	0.36
EQ day	1	18	1.45×10^{-2}	0	0.36
EQ+1 to EQ+6 months	151	15	5.34×10^{-2}	1	0.36

Supplementary figures

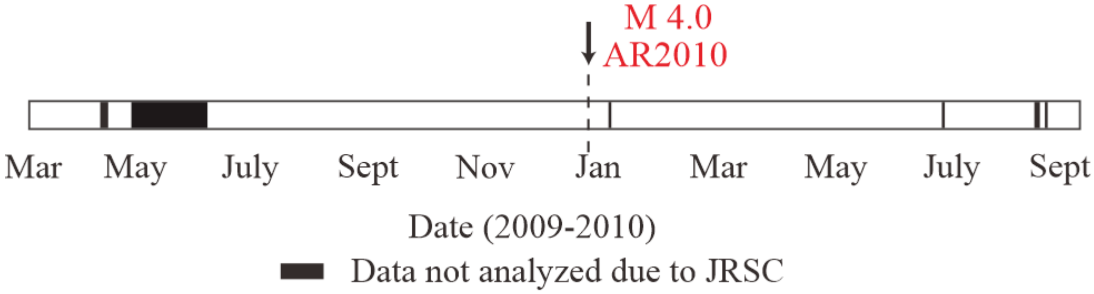

Figure S1: Timeline of data showing data analyzed before and after the 2010 Alum Rock earthquake. Black (bad JRSC data) segments show data not analyzed.

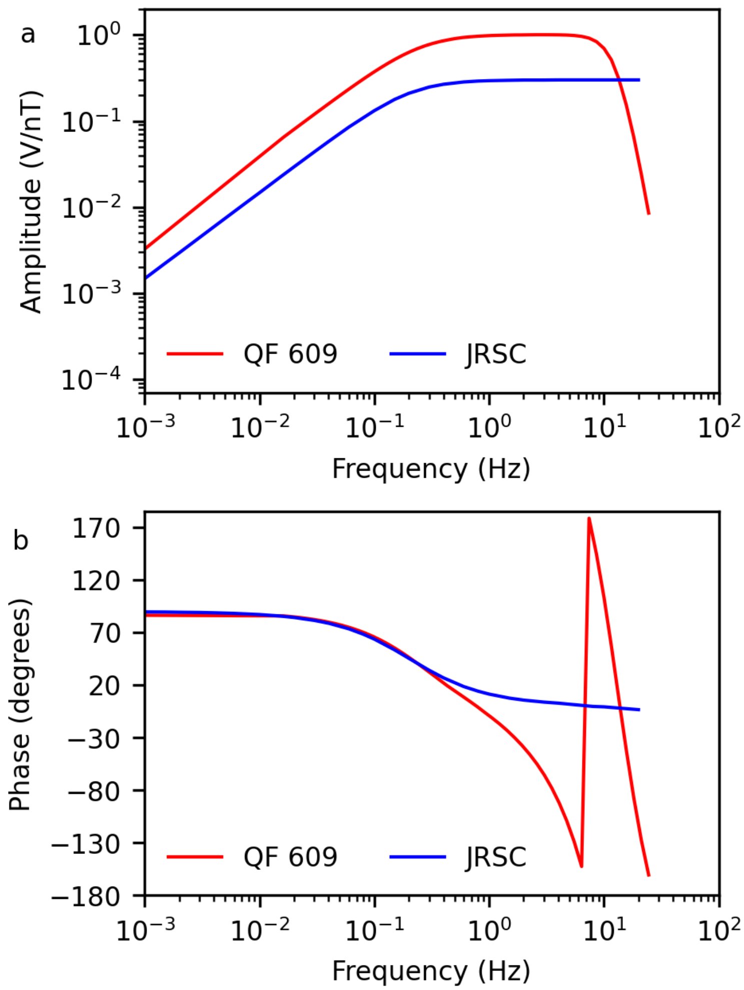

Figure S2: (a) Amplitude spectra and (b) phase spectra of the response function of QF609 and JRSC coils.

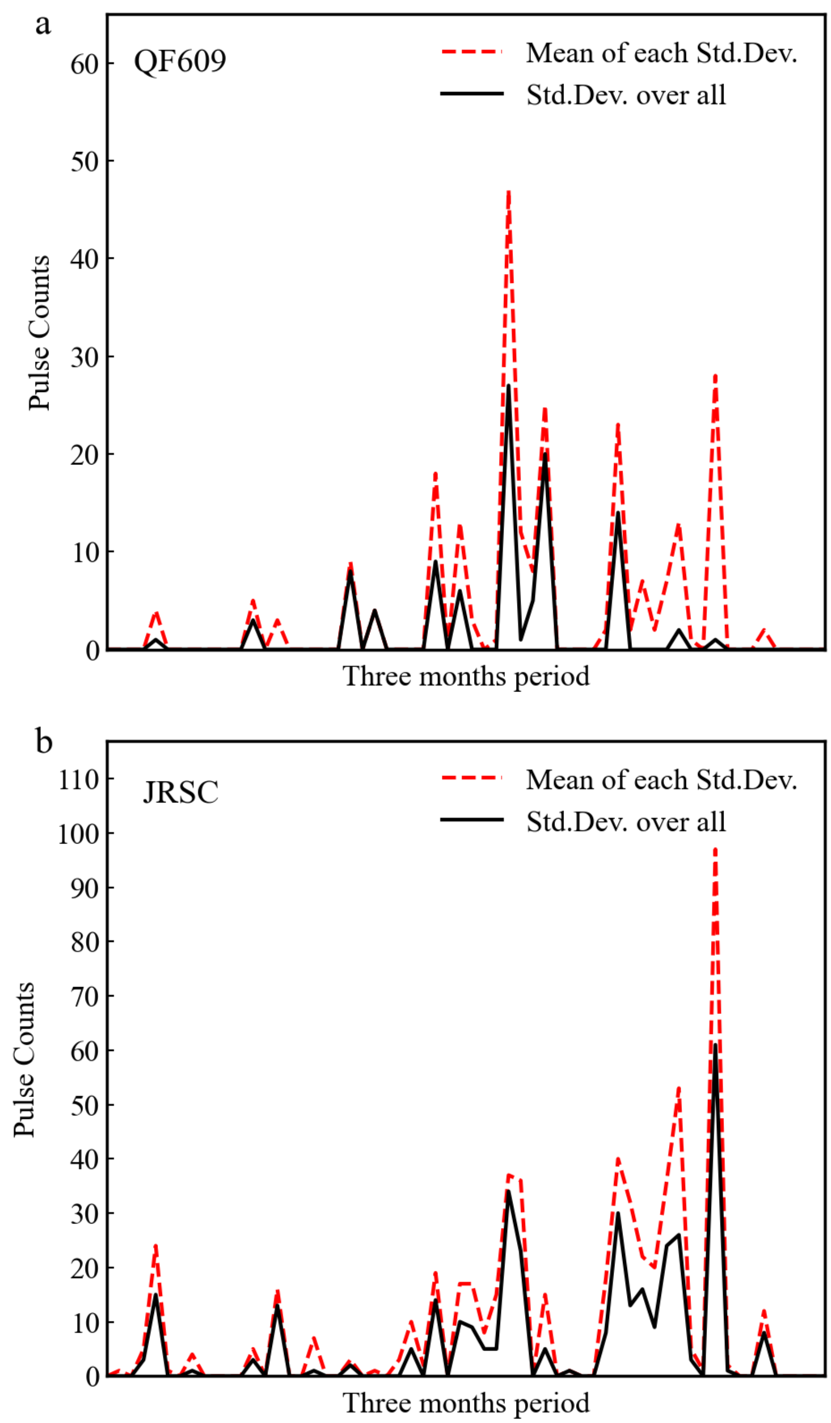

Figure S3: Pulse counts using two different methods to calculate standard deviation, over a ~3-month period, for the east-west magnetometer at (a) QF609 and (b) JRSC. Pulse counts used T=1 s, 4σ threshold. (Black solid curves: pulse counts based on true σ calculated over the entire time period. Red dashed curves: pulse counts utilize an estimate of σ obtained by averaging the true deviation of each day or quiet period.

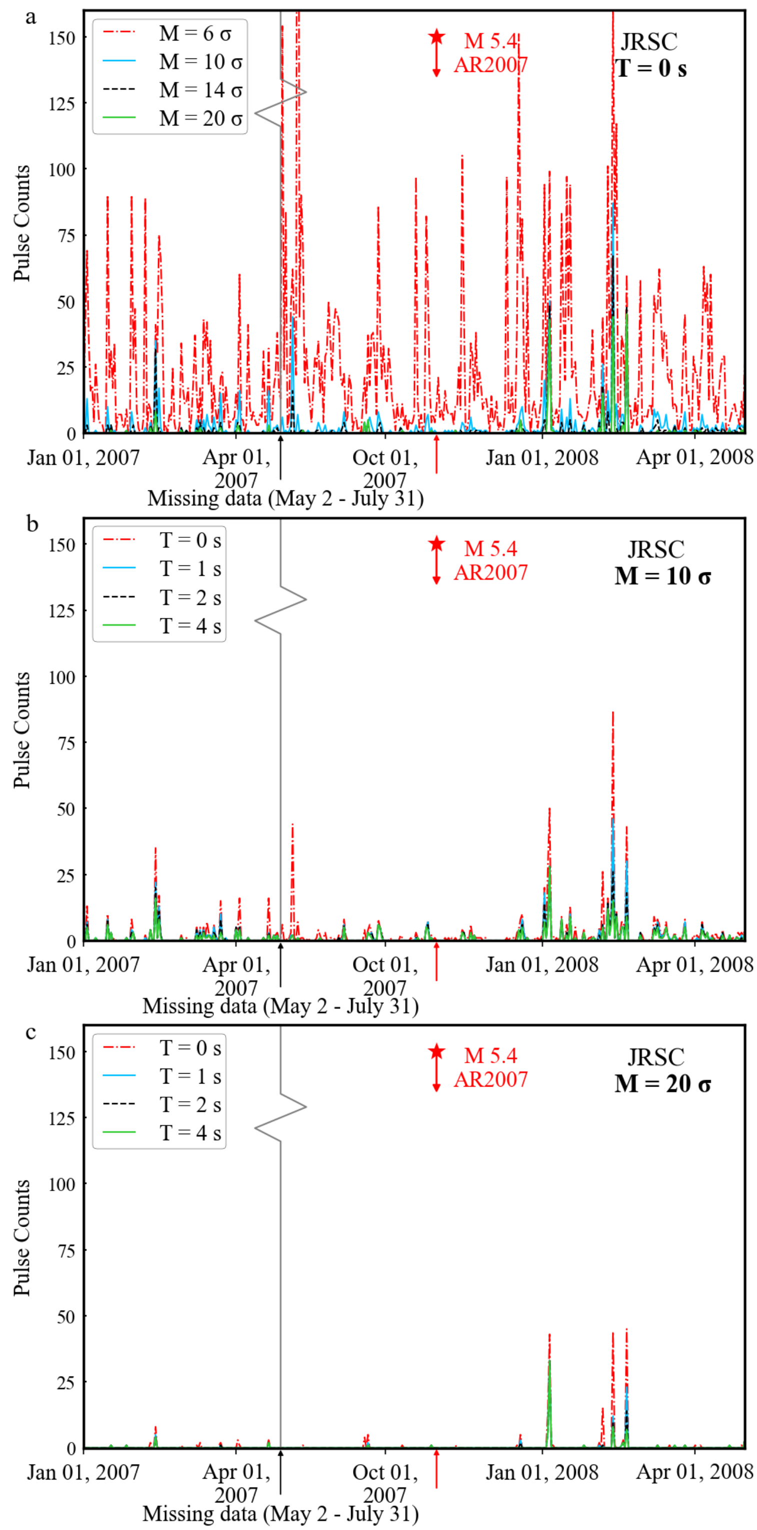

Figure S4: As Figure 6, but for JRSC. Effects of varying parameters on pulse counts for JRSC east-west magnetic coil for 2007–2008. (a) Pulse counts for different thresholds M, with T=0 s. (b) Pulse counts for varying duration parameter T, with M=10. (c) Pulse counts for varying T, with M=20.

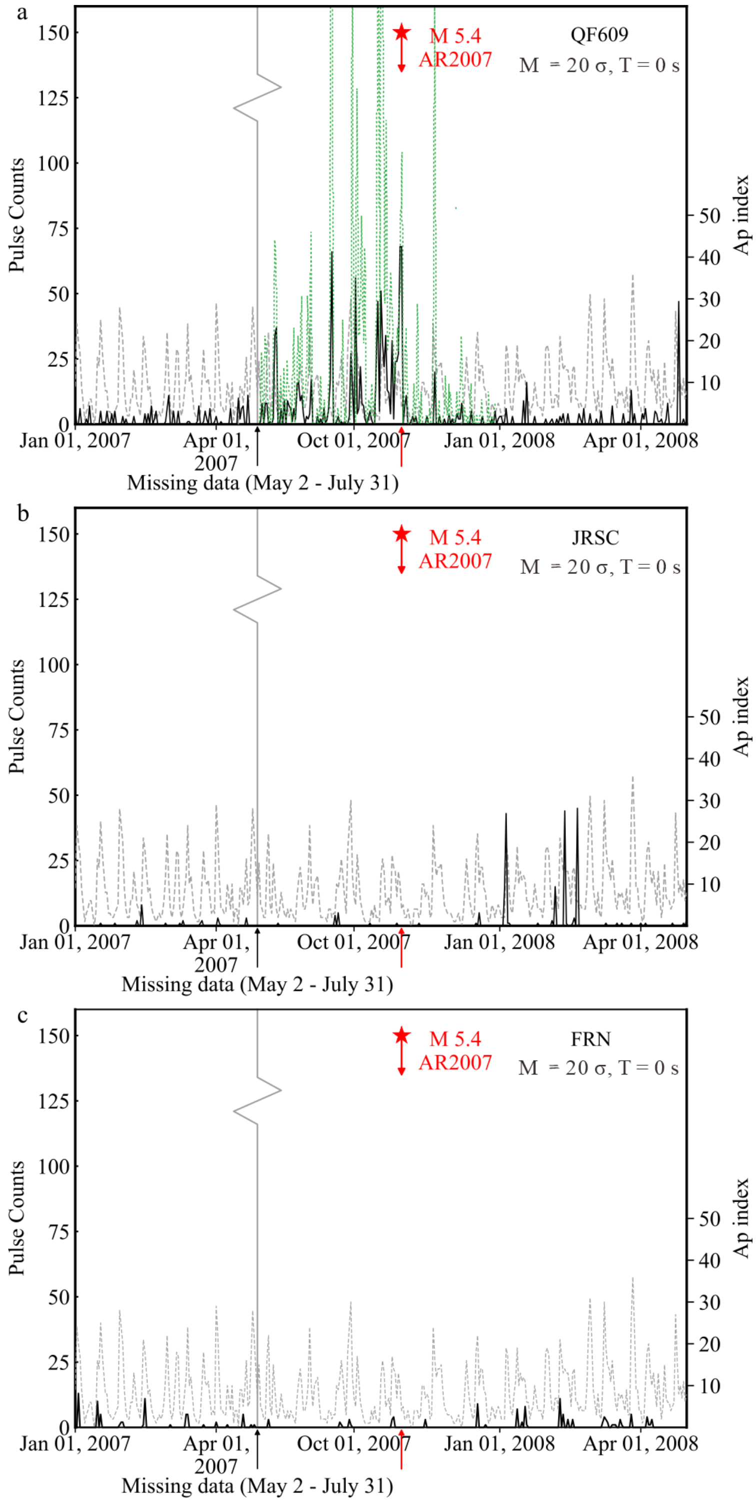

Figure S5: Pulse counts on east-west magnetic channels before and after AR2007, January 1, 2007 to April 30, 2008, made with M=20 σ, T=0 s. (a) QF609; (b) JRSC; (c) FRN. Dashed green lines in part a is the pulse counts for QF609 reported by Bleier et al. (2009). Gray dashed line: Ap index. Red line and star: AR2007 earthquake. (For equivalent figures with M=10 σ, T=0 s, see Figure 7.)

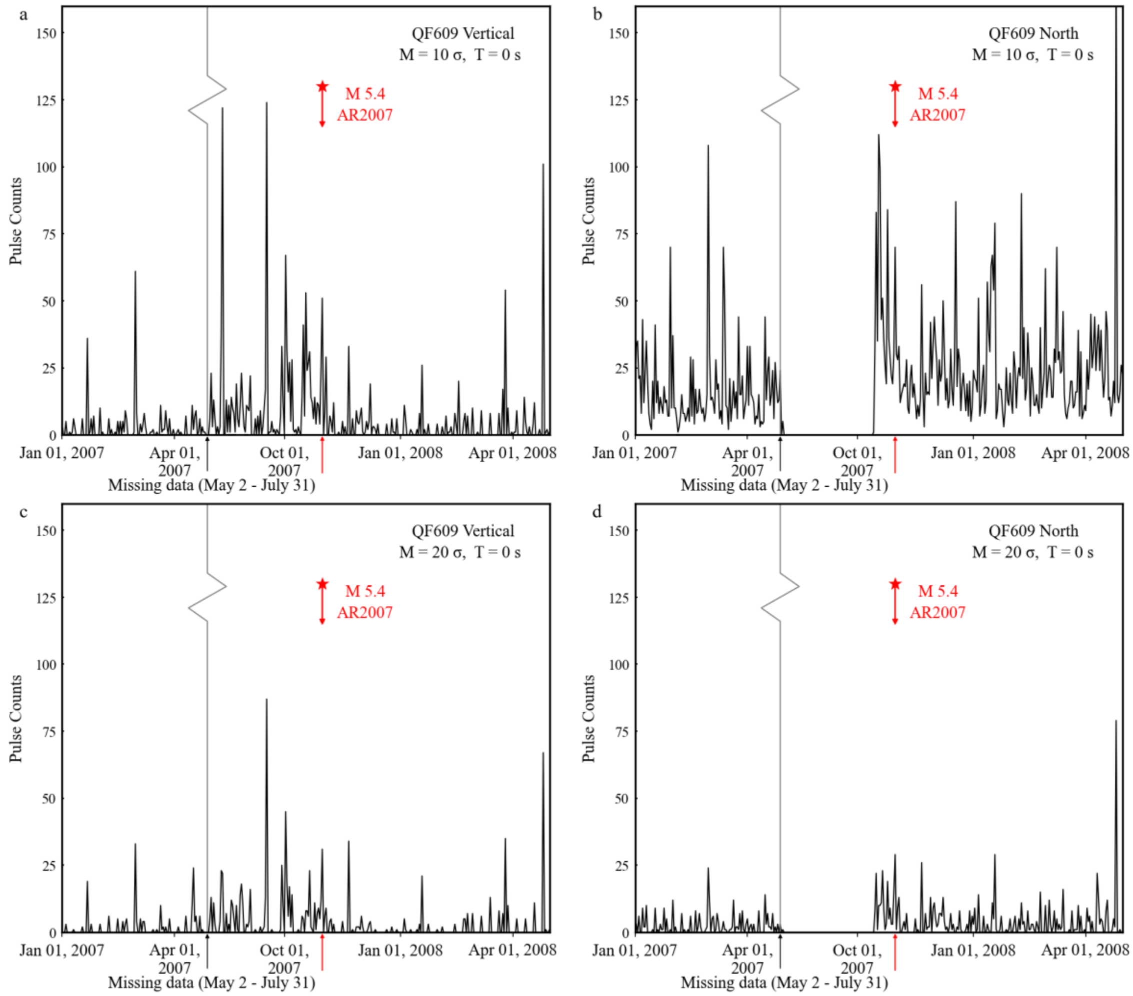

Figure S6: Pulse counts for QF609 north-south and vertical magnetometer channels before and after the 2007 Alum Rock earthquake, January 1, 2007 to April 30, 2008, equivalent to Figures 7 and S5 for the east-west magnetometer. (a) and (c) vertical magnetometer; (b) and (d) north-south magnetometer. (a) and (b) counted with M=10 σ, T=0 s; ((c) and (d) counted with M=20 σ, T=0. AR2007 is indicated by the red line and star.

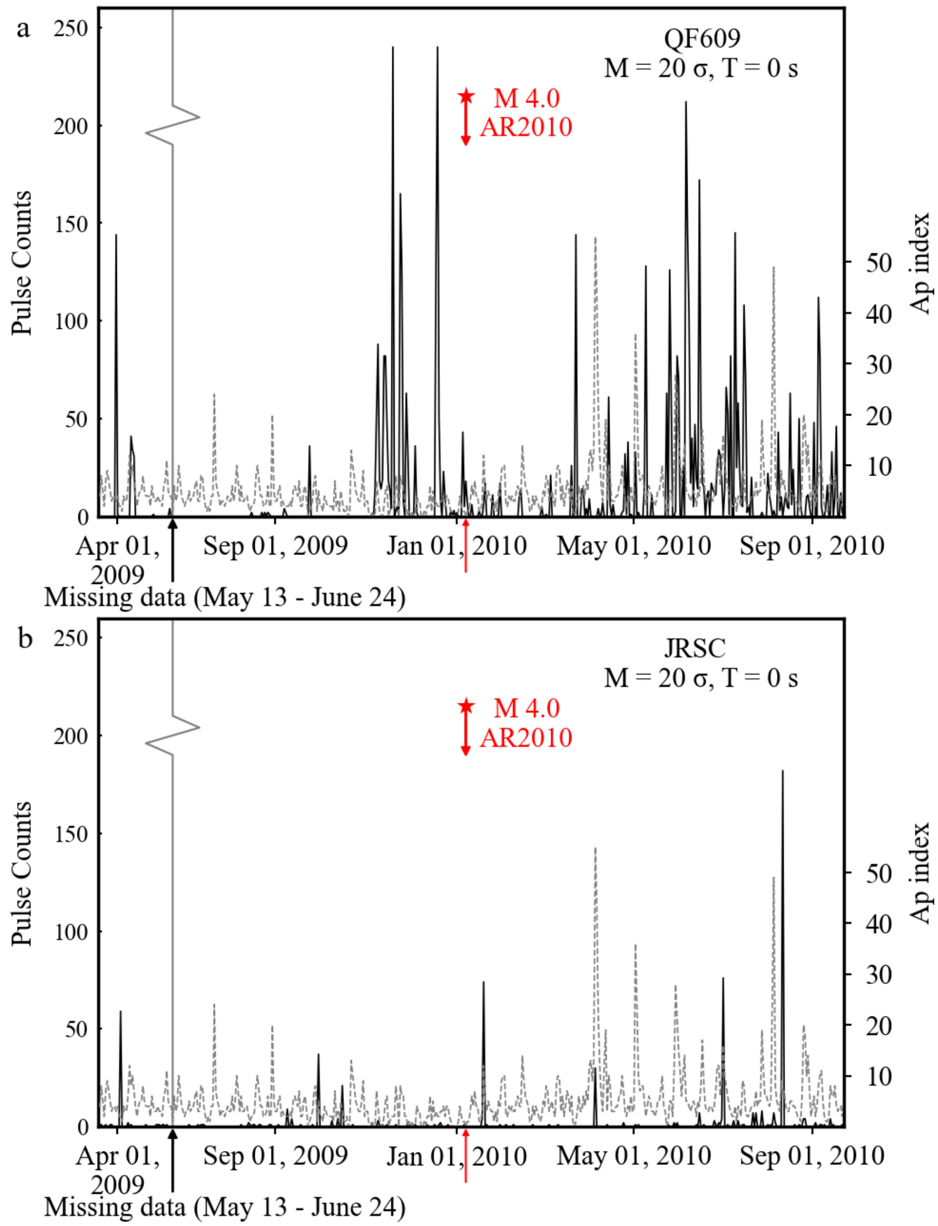

Figure S7: As Figure 8, but with M=20 σ, T=0 s. Pulse counts on east-west magnetic channels before and after the 2010 Alum Rock earthquake, March 19, 2009 to September 24, 2010. (a) QF609; (b) JRSC. Gray dashed line: Ap index. Red line and star: AR2010 earthquake.

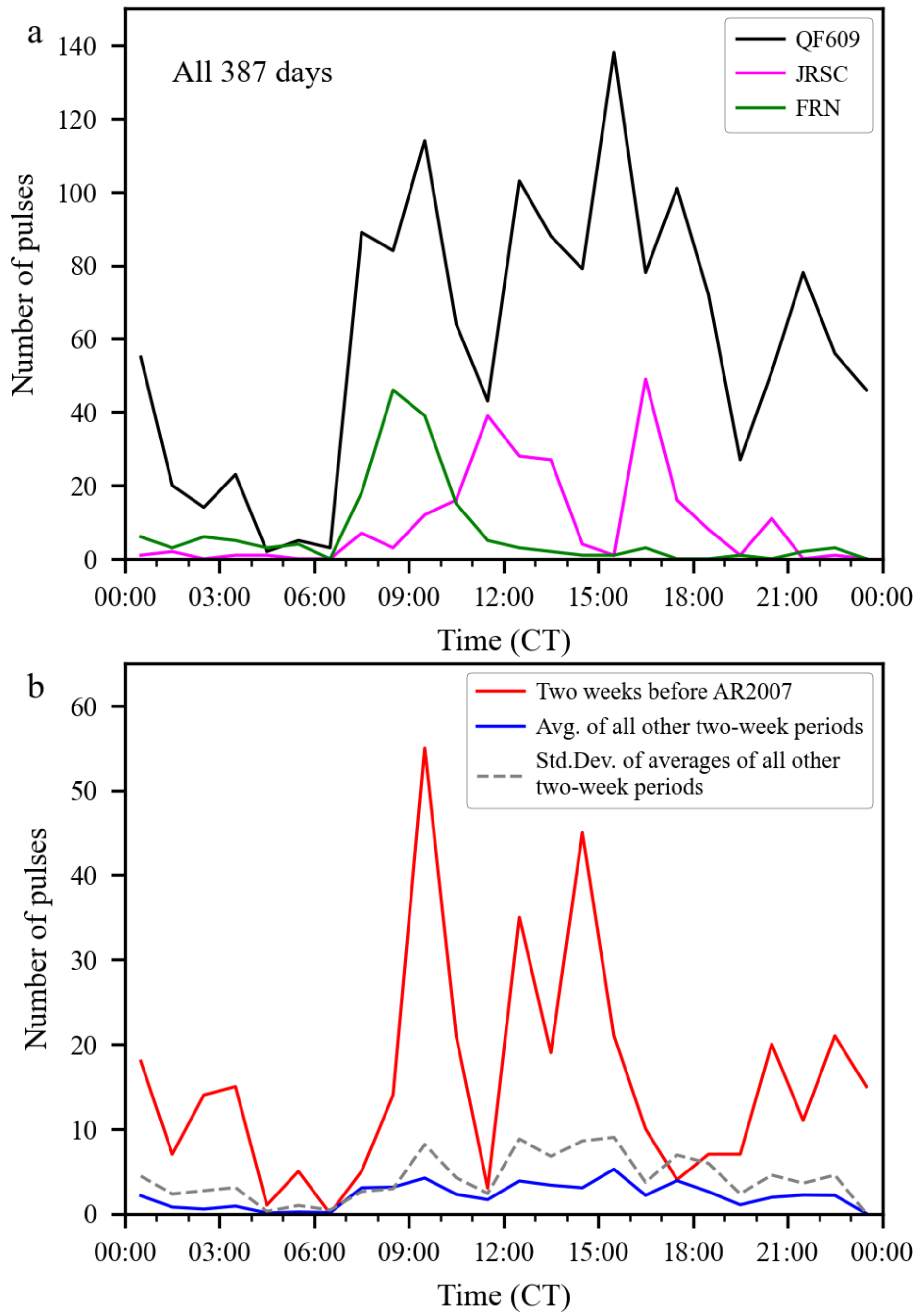

Figure S8: Pulse counts from Fig. S5 (using M = 20 σ, T=0 s) by hour of occurrence (clock time). (a) QF609, JRSC and FRN aggregated over all 387 days; (b) QF609 aggregated over just the two weeks immediately preceding AR2007 (red line) compared to average of pulse counts aggregated over all other two-week periods (blue line) and the standard deviation of these two-week aggregations (gray dashed line) (note change of scale).

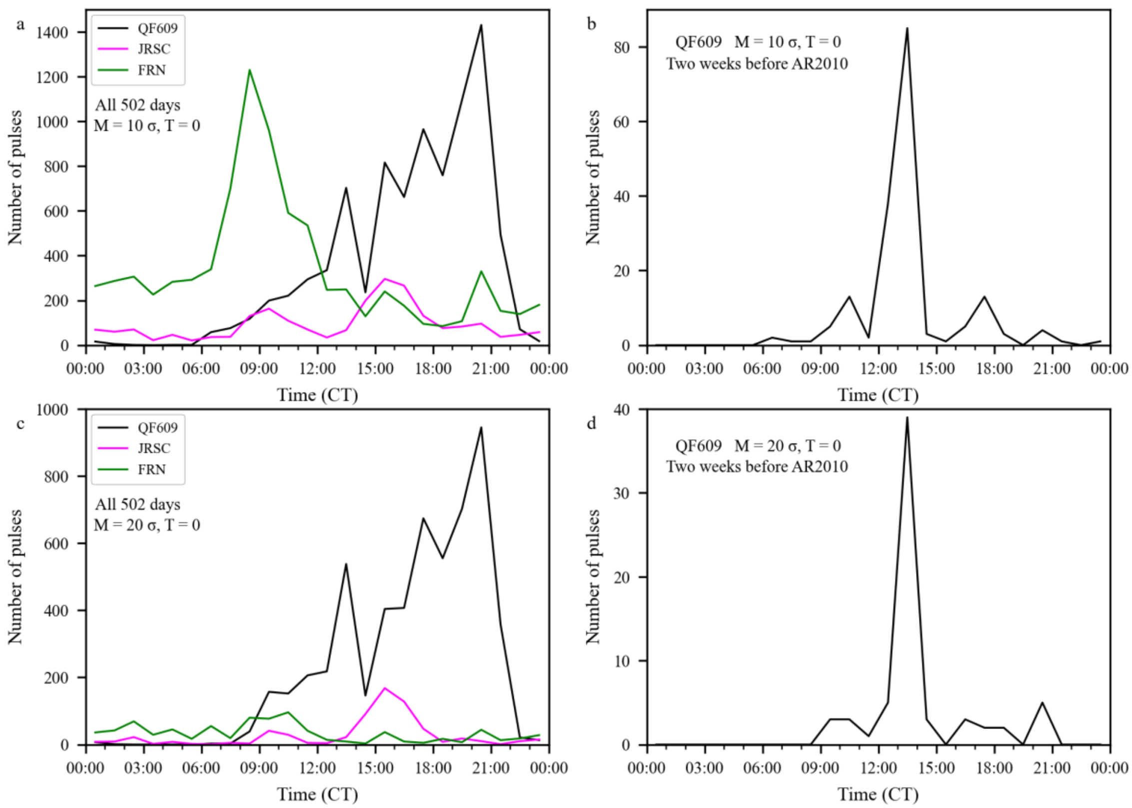

Figure S9: Pulse counts for QF609 for AR2010 from Fig. 8a (parts a and b using M = 10 σ, T=0 s) and Fig. S7a (parts c and d using M = 20 σ, T=0 s) by hour of occurrence (clock time). (a) and (c) aggregated over all 502 days; (b) and (d) aggregated over just the two weeks immediately preceding AR2010.

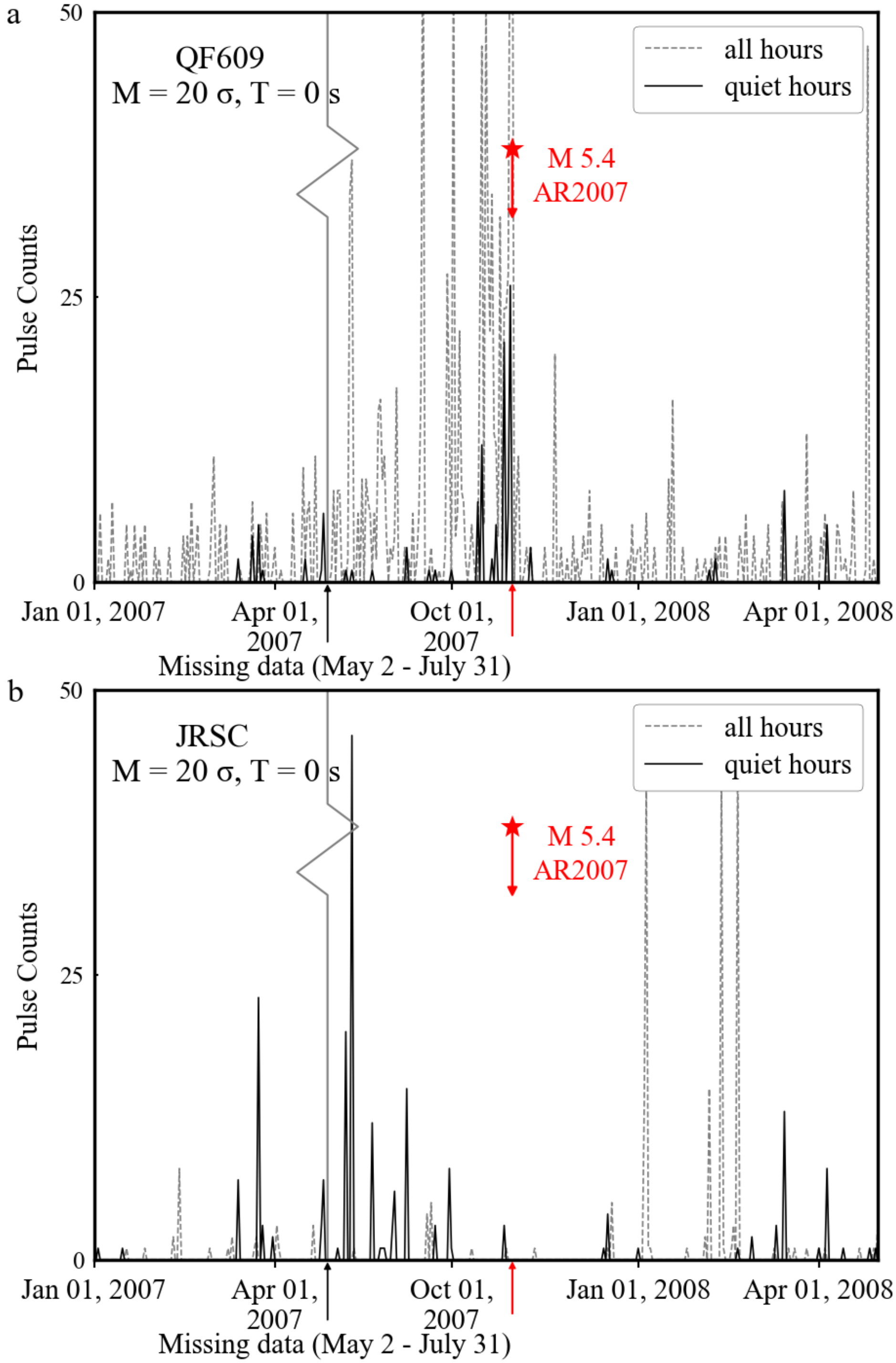

Figure S10: Pulse counts (using M=20 σ, T=0 s) by date for only 02:00–04:00 clock time (solid lines) for (a) QF609 and (b) JRSC compared to 24-hour pulse counts (all hours) from Fig. 8 (gray dashed line). For M=10 σ, T=0 s see Figure 10.

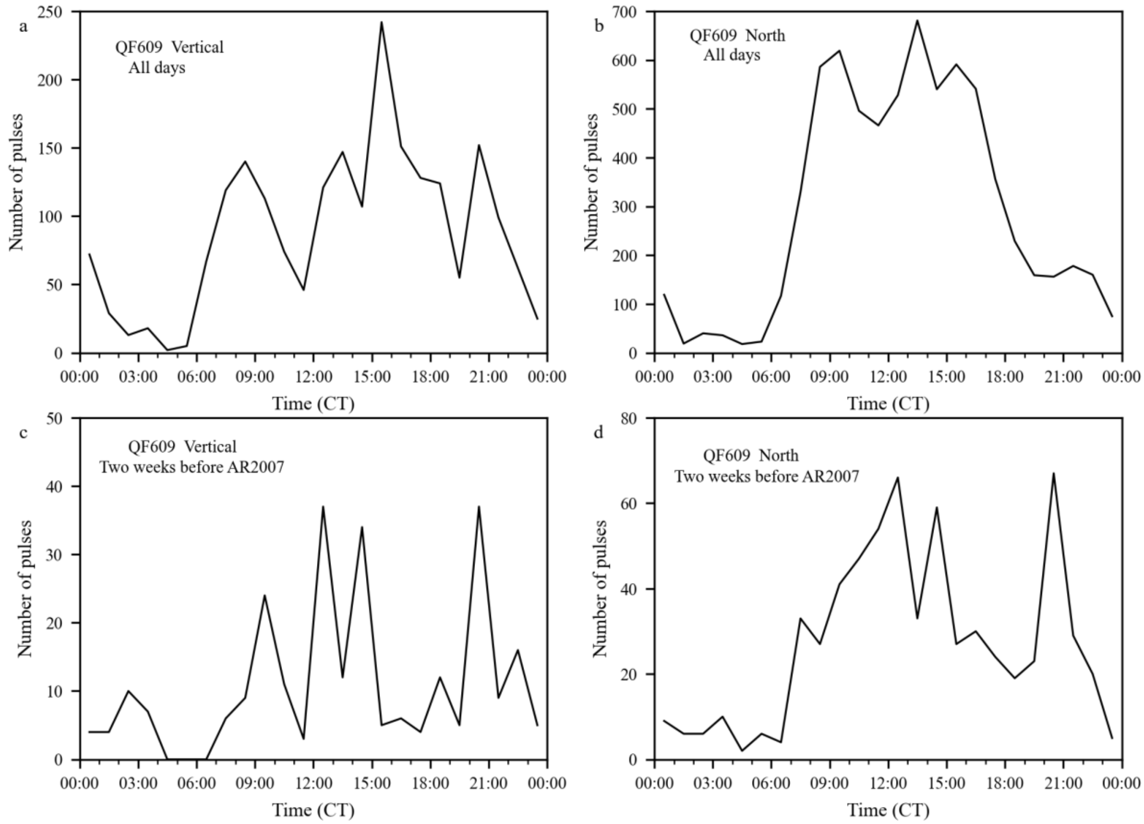

Figure S11: Pulse counts for QF609 north-south and vertical magnetometers (using M=10 σ, T=0 s) by hour of occurrence (clock time). (a) and (c) vertical magnetometer; (b) and (d) north-south magnetometer. (a) and (b) aggregated over all 387 days; (c) and (d) aggregated over just the two weeks immediately preceding AR2007. Equivalent to Figure 9 for QF609 east-west magnetometer.

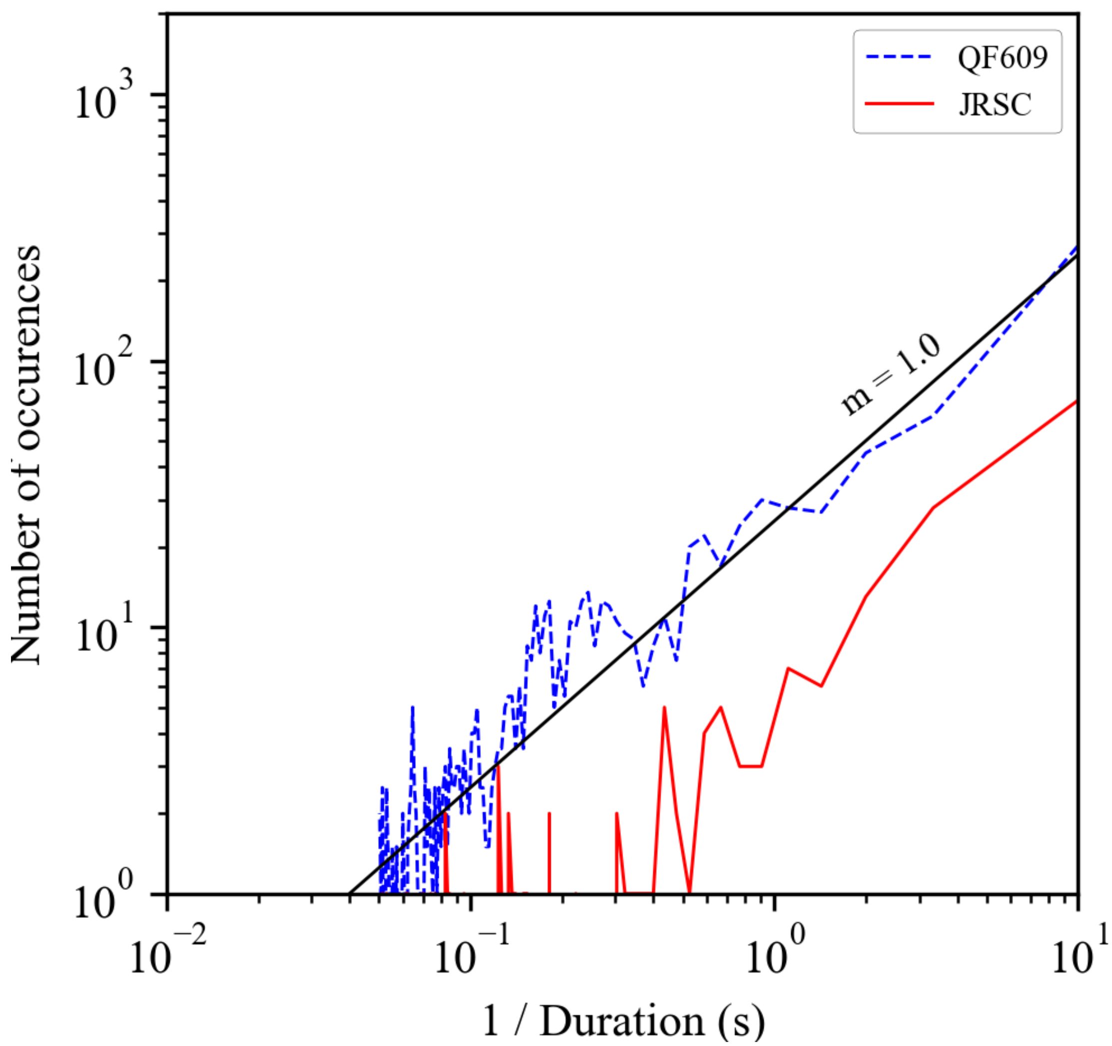

Figure S12: Log number of pulses of specific duration (counted with M=20 σ, T=0) aggregated over all 387 days counted around AR2007 event, plotted against log (reciprocal duration/second), calculated for 0.1 second durations from 0.1–20 s, plotted at bin centers. Dashed blue line: QF609. Solid red line: JRSC. For M=10 σ, T=0 s, see Figure 11.